

USING LIMITED TIME PERIODS AS A MEANS TO EVALUATE MICROWAVE
SOUNDING UNIT DERIVED TROPOSPHERIC TEMPERATURE TREND
METHODS

By

Robb Morris Randall

A Dissertation submitted to the Faculty of the
DEPARTMENT OF ATMOSPHERIC SCIENCES

In Partial fulfillment of the Requirements
For the Degree of

DOCTOR OF PHILOSOPHY

In the Graduate College

THE UNIVERSITY OF ARIZONA

2007

THE UNIVERSITY OF ARIZONA
GRADUATE COLLEGE

As members of the Dissertation committee, we certify that we have read the dissertation

Prepared by Robb Morris Randall

Entitled: Using Limited Time Periods as a Means to Evaluate Microwave Sounding Unit
Derived Tropospheric Temperature Trend Methods

Benjamin M. Herman

Date: JUL 20, 2007

Eric A. Betterton

Date: JUL 20, 2007

Kurtis J. Thome

Date: JUL 20, 2007

Stephen R. Yool

Date: JUL 20, 2007

Xubin Zeng

Date: JUL 20, 2007

Final approval and acceptance of this dissertation is contingent upon the candidate's
submission of the final copies of the dissertation to the Graduate College.

I hereby certify that I have read this dissertation prepared under my direction and
recommend that it be accepted as fulfilling the dissertation requirement.

Dissertation director: Benjamin M. Herman

Date: JUL 20, 2007

STATEMENT BY AUTHOR

This dissertation has been submitted in partial fulfillment of requirements advanced degree at the University of Arizona and is deposited in the University of Arizona and is deposited in the University Library to be made available to borrowers under rules of the library.

Brief quotations from this dissertation are allowable without special permission, provided that accurate acknowledgment of source is made. Requests for permission for extended quotation from or reproduction of this manuscript in whole or in part may be granted by the head of the major department or the Dean of the Graduate College when in his or her judgment the proposed use of the material is in the interests of scholarship. In all other instances, however, permission must be obtained from the author.

SIGNED: _____
Robb Morris Randall

The views expressed in this article are those of the author and do not reflect the official policy or position of the United States Air Force, Department of Defense, or the U.S. Government

ACKNOWLEDGMENTS

I would like to thank first and foremost God for using me in ways He deems necessary. My wife, for the love and support in our journey, and my children for being a guiding light to all that is right. The folks God has put in my path: My advisor, Professor Ben Herman; as his most recent last student I am thankful, blessed and honored to have been able to be mentored by the best. My Minor advisor, Professor Kurtis Thome; his guidance and mentoring were invaluable and paramount for my timely completion. The rest of my committee; Professors Eric Betterton, Xubin Zeng and Stephen Yool whose guidance and time can't be more appreciated. Angel Otárola; his friendship and spiritual guidance on a daily basis were invaluable. Drs John Christy, Carl Mears, Roger Pielke Sr., William Randel, Dale Ward I thank for their insightful comments and generous offer of data used in this work. The entire staff and graduate students at the Department of Atmospheric Sciences at the University of Arizona also garner much appreciation as each of them is present in this work.

TABLE OF CONTENTS

LIST OF FIGURES	8
LIST OF TABLES	12
ABSTRACT	13
CHAPTERS	
1 INTRODUCTION	15
1.1 Introduction.....	15
1.2 Background History.....	19
2 MICROWAVE SOUNDING UNIT OVERVIEW.....	23
2.1 Sensor specifics.....	23
2.2 Weighting Functions.....	24
3 DATA.....	29
3.1 Satellite.....	29
3.2 Radiosonde.....	29
3.3 Surface.....	30
3.4 Limited Time Periods.....	30
4 STATISTICAL METHODS EVALUATION USING LIMITED TIME PERIODS.....	33
4.1 Introduction.....	33
4.2 RATPAC(RW) Limited Time Period Trends / Zero Trend Level.....	34
4.3 Review of JF06 regression method.....	40
4.4 methods of regression using LTP analysis.....	41
4.4.1 RH07.....	41
4.4.2 JF06NEW.....	44
4.4.3 NoCONST.....	44
4.5 Results of regression methods using LTP.....	51
4.6 Additional issues with using MT and LS combination.....	62

TABLE OF CONTENTS – *Continued*

4.6.1 MSU Instrumentation.....	62
4.6.2 Static weighting function.....	62
4.7 Summary and Conclusions.....	63
5 LIMITED TIME PERIOD COMPARISON OF UAH/RSS.....	65
5.1 Introduction.....	65
5.2 Methods.....	66
5.3 Results and Attribution.....	69
5.3.1 Review in correction/merging methods.....	69
5.3.2 Results and Attribution.....	71
5.4 Radiosonde Comparison.....	81
5.5 Summary and Conclusions.....	87
6 ATMOSPHERIC AMPLIFICATION.....	91
6.1 Globally Averaged Atmospheric Amplification.....	91
7 SUMMARY AND CONCLUSIONS.....	96
7.1 Summary and Conclusions.....	96
7.2 Future Work.....	99
REFERENCES	101

LIST OF FIGURES

FIGURE 2.1, MSU Weighting functions	28
FIGURE 4.1, MSU LS and MT weighting function intersection.....	36
FIGURE 4.2, 15-year LTP trends on RATPAC(RW).....	37
FIGURE 4.3, 20-year LTP trends on RATPAC(RW).....	38
FIGURE 4.4, 25-year LTP trends on RATPAC(RW).....	39
FIGURE 4.5, MSU MT and LS Weighting functions indicating layers used in statistical methods to eliminate stratospheric temperature.....	43
FIGURE 4.6, aLS, aMT coefficients found using least squares regression at each 15- year LTP.....	47
FIGURE 4.7, aLS, aMT coefficients found using least squares regression at each 20- year LTP.....	48
FIGURE 4.8, aLS, aMT coefficients found using least squares regression at each 25- year LTP.....	49
FIGURE 4.9, Various methods of creating coefficients from RATPAC(RW) radiosonde data and corresponding T_{TR} were created using equation (4.1). These were subtracted from the actual T_{TR} found using equation (4.2) for 15- year LTP over the entire radiosonde time period. (b) Over the MSU era.....	56

LIST OF FIGURES – *Continued*

- FIGURE 4.10, Various methods of creating coefficients from RATPAC(RW) radiosonde data and corresponding T_{TR} were created using equation (4.1). These were subtracted from the actual T_{TR} found using equation (4.2) for 20-year LTP over the entire radiosonde time period. (b) Over the MSU era..... 57
- FIGURE 4.11, Various methods of creating coefficients from RATPAC(RW) radiosonde data and corresponding T_{TR} were created using equation (4.1). These were subtracted from the actual T_{TR} found using equation (4.2) for 25-year LTP over the entire radiosonde time period. (b) Over the MSU era..... 58
- FIGURE 4.12, Various methods of creating coefficients, were applied to 15-year LTP trends from RATPAC(RW) radiosonde data and corresponding T_{TR} were created using equation (4.1). These were subtracted from T_{TR} found using RH07 and the difference of trends is shown..... 59
- FIGURE 5.1, (a) RSS(MT)-UAH(MT) (grey offset by 1.0) and RSS(LT)-UAH(LT) (black offset by 0.5) temperature difference anomaly time series for global data over land, (b) tropical data over land. (c) 10-year Limited Time Period (LTP) trends of difference time series for global data; LT(dashed) MT(solid), (d) tropical data LT(dashed) MT(solid). (e) 5-year LTP trends of the difference time series for global data; LT (dashed) MT(solid), (f) tropical data; LT (dashed) MT(solid)..... 68
- FIGURE 5.2, 10-year LTP global trends for the RSS(LT)-UAH(LT) difference series over ocean (dashed) and land (solid)..... 74

LIST OF FIGURES – *Continued*

- FIGURE 5.3, RSS(LT)-UAH(LT) (a) Global difference time series (RSS(LT)-UAH(LT)) over land 1989-1999 (b) Tropical difference time series over land 1998-2003. (c) RSS global average diurnal correction for NOAA-11(black) and NOAA-12(grey) 1989-1999. (d) RSS global average diurnal correction for NOAA-14 1998-2003..... 75
- FIGURE 5.4, (a) Limited Time Period (LTP) trends on RSS(MT)–UAH(MT) (solid) and RSS(LT)-UAH(LT) (dashed) for 10-year LTP global land, (b) ocean. (c) 5-year LTP global land and (d) ocean..... 77
- FIGURE 5.5, (a) 10-year LTP trends on UAH(LT)-UAH(MT) (solid) and RSS(LT)–RSS(MT) (dashed) for global, (b) tropics. (c) and (d) same as (a) and (b) for 5-year LTP trends. 79
- FIGURE 5.6, (a) 10-year LTP trends on UAH(LT)-UAH(MT) (solid), RSS(LT)–RSS(MT) (grey) and Sonde(LT)-Sonde(MT) (dashed). (b) Same as (a) with 5-year LTP trends 83
- FIGURE 5.7, (a) Differences from series types created in Figure 5.6. 10-year LTP trends for RSS-Sonde (global, land) and (b) Sonde-UAH. Dashed lines around each are the 95% CI. 85
- FIGURE 5.8, (a) Differences from series types created in Figure 5.6. 5-year LTP trends for RSS-Sonde (tropics, land) and (b) Sonde-UAH. Dashed lines around each are the 95% CI 86

LIST OF FIGURES – *Continued*

- FIGURE 6.1, 25-year LTP for various estimated troposphere temperature trends. GHCN-ERSST and HadCRUTv2 surface 25-year trends are shown for comparison 94
- FIGURE 6.2, 25-year LTP trends (K/decade) centered on 1975-1994.5 for a atmospheric layer 1000-200 hPa. Greatest warming is ~ 300-500 hPa; over the MSU era, trends centered on 1991.5-1994.5 one would not see atmospheric amplification..... 95

LIST OF TABLES

TABLE 3.1, Radiosonde sites used in this study 32

TABLE 4.1, Techniques used to calculate globally averaged regression coefficients 50

ABSTRACT

Limited Time Period (LTP) running trends are used to evaluate Microwave Sounding Unit (MSU) derived tropospheric temperature trend methods in an attempt to alleviate documented considerable disagreements between tropospheric datasets so investigation into the atmospheric variability is able to move forward.

Regression derived coefficients were used to combine lower stratosphere (LS) and mid-troposphere to lower stratosphere (MT) simulated MSU channels from RATPAC radiosonde data. This protocol is used to estimate tropospheric temperature trends and compared to actual RATPAC derived tropospheric temperature trends. It is found that the statistical LS/MT combination results in greater than 50% error over some LTP. These errors are found to exist when strong cooling in the stratosphere is coincident with periods when the level separating cooling from warming is above the tropopause.

LTP trends are also created from various MSU difference time series between the University of Alabama in Huntsville (UAH) and Remote Sensing System (RSS) group's lower troposphere (LT) and MT channels. Results suggest the greatest discrepancies over time periods where NOAA-11 through NOAA-15 adjustments was applied to the raw LT data over land. Discrepancies are shown to be dominated by differences in diurnal correction methods due to orbital drift. Comparison of MSU data with radiosonde data indicate that RSS's method of determining diurnal effects is overestimating the correction in the LT channel. Diurnal correction signatures still exist in the RSS LT time series and are likely affecting the long term trend with a warm bias.

These findings suggest atmospheric amplification is not happening in the atmosphere using globally averaged data over the MSU era. There is evidence however from the radiosonde data that shows greater warming in the ~300-500 hPa layer than at the surface during some LTP in the complete radiosonde database. This temporal change in temperature trends warrants further studies on this subject.

This research suggests overall that the temporal changes in temperature trend profiles and their causes are extremely important in our understanding of atmospheric changes and are themselves, not well characterized.

CHAPTER 1

INTRODUCTION

1.1 Introduction

Accurate assessment of satellite derived temperature trends in the atmosphere is paramount to our understanding of climate change. The Microwave Sounding Unit (MSU) derived atmospheric temperature trends are used in various climate studies for model verification [*Vinnikov, et al., 2006*], to infer trends in other atmospheric parameters [*Soden, et al., 2005*], to derive trends in atmospheric layers not directly obtained from the MSU [*Johanson and Fu, 2006*] and to provide evidence of changes in planetary-scale atmospheric circulation [*Fu, et al., 2006*], to name a few. The resultant MSU derived global and tropical atmospheric trends themselves have received the most attention. These trends are at the center of determining whether amplification (greater warming in the troposphere than at the surface) of temperature trends in the atmosphere exists as prescribed by climate models and the current understanding of the atmospheric physics [*Christy, et al., 2007; Karl, et al., 2006; Santer, et al., 2005*].

The MSU data suffer from a number of calibration issues and time-varying biases that must continue to be addressed as they are used for climate change studies [*Mears and Wentz, 2005*]. Additionally, the accuracy of methods that combine different MSU channel data to obtain tropospheric trends is still debated in the scientific literature [*Johanson and Fu, 2006; Spencer, et al., 2006*]. Although the MSU wasn't originally meant for climate studies [*Christy, et al., 2003*] it is used extensively for this purpose and

a thorough examination of the data and applications are necessary to ensure long-term stability as required for climate change studies.

Currently three separate groups derive multiple temperature databases directly from satellite based MSU radiance measurements: the University of Alabama in Huntsville (UAH), Remote Sensing System (RSS) and the University of Maryland (UMd). RSS and UAH produce temperature products for three layers; the mid troposphere to lower stratosphere (termed MT), roughly, surface to 75 hPa; the lower stratosphere (termed LS), roughly 150 to 15hPa (see Figure 2.1); and the lower troposphere (termed LT) , roughly surface to 300 hPa; [Christy and Norris, 2006]. The LT channel, used by RSS and UAH, is produced by a linear combination of MT channels viewing at different zenith angles. UMd produces a temperature product for MT only. Additionally, Fu et al., [2004a] (hereafter FJWS) derived a method that uses linear regression with radiosonde data to create coefficients that remove the stratospheric influence from the MT channel using a linear combination of the LS and MT channel. The resultant tropospheric layer is roughly surface to 150hPa and is termed T_{tr} [Johanson and Fu, 2006] (hereafter JF06).

Each group's database produces different temperature trends for their respective channels (MT, LT, T_{tr}). The differences can be categorized in two ways. First, there are differences in procedures between the groups that use the MSU raw data to create time series and temperature trends. Differences in these satellite estimates of trends are caused by each group using different processes in merging data from the individual satellites used in the time series and differences between the diurnal adjustments that are used to

account for orbital drift of the satellite [Mears, et al., 2006]. Second, there are differences between the trends derived by methods from Johanson and Fu [2006] (JF06) and those from raw MSU data. Differences in these trend estimates (other than the aforementioned) are caused by the different layers represented in the time series and the accuracy in which the JF06 method is able to remove the stratospheric influence from the MT channel using the LS channel.

Recent studies have documented differences between the UAH and RSS data sets and find that the likely primary cause of differences between the two groups (i.e., UAH, RSS) in the LT and MT channels are the on-board calibration target parameters calculated by each group due to different choices of overlap periods of the satellites used to create the time series [Christy and Norris, 2006; Christy, et al., 2007; Mears, et al., 2006; Mears and Wentz, 2005]. Methods to determine diurnal correction are found to be a secondary issue. The United States Climate Change Science Program's (CCSP) *Temperature Trends in the Lower Atmosphere: Steps for Understanding and Reconciling Differences* [Karl, et al., 2006] addressed discrepancies in satellite trends and methods for creating temperature anomaly time series. Their recommendation is to diagnose the relative merits of different merging methods for satellite data over limited time periods where the largest discrepancies between satellites and radiosonde data are found [Mears, et al., 2006].

Other studies have debated the validity of JF06 method for removing stratospheric influence from the MT channel using the LS channel [Fu and Johanson, 2005; Fu, et al., 2004a; Johanson and Fu, 2006; Spencer, et al., 2006]. This debate is still active,

however all databases (UAH, RSS, JF06) are used in the CCSP report to determine if amplification in the atmosphere as seen from observations is consistent with that produced by climate models. Due to these inconsistencies the CCSP concludes:

“..due to the considerable disagreements between tropospheric datasets, it is not clear whether the troposphere has warmed more than or less than the surface”

A linear fit over the entire time period to compare long term trends may not be the best technique to compare the databases in order to diagnose differences between derived temperature trends as have been done in the past. Comparing the data over shorter, or limited time periods (LTP), affords the opportunity to determine how methods affect data for the actual time period over which differences in merging methods are used. The use of LTP to create coefficients also helps to more accurately determine the merits of the methods. Thus, any similar discrepancies among the methods found at more than one LTP could be resolved in a single process used over those time periods. These similar discrepancies may not be seen using one long term linear trend. Furthermore some changes in climate forcing (e.g., stratospheric ozone, solar radiation, methane) have occurred over a time period shorter than the entire 28-year MSU period. These forcings over LTP have led to temperature changes in the atmosphere over LTP, thus need to be analyzed in the same manner to understand the complex feedback processes.

The objective of this study is to evaluate MSU derived temperature trend methods in an attempt to illuminate the causes of “the considerable disagreements between tropospheric datasets” (CCSP) so investigation into the atmospheric variability is able to move forward. In order to properly introduce the importance of this study, the rest of

Chapter 1 will detail background information into the role of tropospheric temperature trends in the quest for answers on atmospheric amplification. An overview of the MSU instrument is provided in Chapter 2 and the data used is described in Chapter 3.

Investigating statistical methods from MT and LS channels using LTP is described in Chapter 4 of this study. As recommended by the CCSP investigation of the largest discrepancies between MSU data sets is described in Chapter 5. A brief look into how the findings relate to atmospheric amplification is discussed in Chapter 6. Summary, Conclusions and future work will be laid out in Chapter 7.

1.2 Background

Modeled and observed tropospheric trends are claimed to be fundamentally inconsistent. Santer et al., [2000] found that modeled surface and MSU LT channel [Christy, et al., 2000] trends were close enough to be considered consistent. However, they also found when surface – LT modeled trends were compared to surface – LT observed trends there were significant differences, indicating theoretically based atmospheric amplification (warming greater in the troposphere than at the surface) was not represented by observations. The UAH group created the LT channel (a linear combination of the MT channel at different view angles) to alleviate, at the time, the warming influence of the stratosphere on the MT channel. Subsequently Prabhakara et al., [2000] created an MT channel data base obtaining a trend of 0.13 K/decade for a time period of 1980-1999.

Further calibration adjustments were accomplished on the raw MSU data produced by the UAH group, resulting in MT and LT trends of 0.02 K/decade and 0.06

K/decade respectively for 1979-2002 time period [Christy, et al., 2003; Zou, et al., 2006]. The small trends were inconsistent with the larger trends of about 0.17 K/decade obtained from surface observations [Folland, et al., 2001]. Due to this apparent discrepancy Mears et al., [2003] reanalyzed the MSU raw data and created a new MT channel database by using different merging techniques than the UAH group. Their MT database showed a 0.10 K/decade warming for a time period of 1979-2001. Although this was closer to the surface trend and consistent with Prabhakara et al., [2000], it still indicated that observations were not showing atmospheric amplification over the MSU time period.

FJWS developed a statistical method using linear regression to combine the MT and LS channels to eliminate the stratospheric influence on the MT channel. Their method, modified in JF06, estimates the tropospheric temperature trend for a layer from the surface to the tropopause, instead of surface to ~400-500hPa that the LT channel represents. Their results indicate more warming in the troposphere and produce temperature trends that are near or greater than the surface trend for the RSS database but still less than the surface trends using the UAH database.

Vinnikov, et al., [2006] created yet another MT database using differing satellite diurnal cycle corrections than RSS and UAH and found that the globally averaged trend for a time period of 1978 – 2004 was 0.20 K/decade which compared very well with the trend obtained from surface reports. Their method, however, only removed the first harmonic of the diurnal cycle while UAH and RSS remove first and second harmonics in their corrections, indicating a likely source of errors in the Vinnikov, et al., [2006] database [Mears, et al., 2006].

Mears and Wentz [2005] developed an LT channel so comparisons with UAH data became available. In the same work they found an error in the UAH tropical LT calculations; corrections slightly increased the trends in the effected channel. A subsequent study was done by Santer, et al., [Santer, et al., 2005] using the RSS and UAH MT and LT channels, to determine atmospheric amplification in the tropical atmosphere. Findings indicated that the only database that agreed with the modeled amplification was the RSS database.

The United States Climate Change Science Program (CCSP) comprehensive report: *Temperature Trends in the Lower Atmosphere: Steps for Understanding and Reconciling Differences* [Karl, et al., 2006] found:

“Since the late 1950’s, all radiosonde data sets show that the low and mid troposphere have warmed at a rate slightly faster than the rate of warming at the surface for global-average. For observations during the satellite era (1979 onwards), ... the majority of these data sets show warming at the surface that is greater than in the troposphere...some datasets show the opposite. ...Some climate model simulations show more warming in the troposphere than at the surface, while a slightly smaller number of simulations show the opposite behavior. There is not fundamental inconsistencies among these model results and observations at the global scale.”

Most important to the present work:

“Thus, due to the considerable disagreements between tropospheric datasets, it is not clear whether the troposphere has warmed more than or less than the surface”

One of the recommendations is to diagnose the relative merits of different merging methods for satellite data over limited time periods where the largest discrepancies between satellites and radiosonde data are found. My work takes this recommendation one step further and uses LTP to evaluate all of the MSU derived temperature trend methods, using the newest globally homogenized radiosonde database available.

CHAPTER 2

MICROWAVE SOUNDING UNIT

2.1 Sensor Specifics

The microwave sounding unit (MSU) on the NOAA polar orbiting environmental satellites (POES) is a Dicke-type passive radiometer with four channel frequencies centered in the 50 to 60GHz oxygen absorption complex (50.30, 53.74, 54.96, and 57.95 GHz) [Mo, *et al.*, 2001]. A cross-track rotating reflector directs the incoming radiation through a fixed circular horn coupled to the radiometers. The antenna beamwidths are both set to 7.5° by the reflector dimensions (~ 6 cm). This results in a 3 dB (half-power) footprint at nadir of 110km for the 833km polar orbiting altitude. Half-power beamwidth is defined by the points on the sides of the antenna main lobe where the received energy is 50% of that at the lobe center. Due to the increasingly oblique viewing off-nadir, combined with the curvature of the earth, footprints off-nadir increasing horizontal sizes [Grody, 1983]. The 11-footprint scan lines are repeated every 25.6 seconds providing 170 km spacing between scan lines. The 7.5° beam width from the satellite orbital altitude of approximately 850km results in an atmospheric footprint horizontal size (spatial resolution) at nadir of about 110km (circular), increasing to about 180km by 320km (elliptical) at the scan extremes. In contrast to the point measurement of a thermometer, the horizontal and vertical sampling of each MSU measurement represents approximately $100,000 \text{ km}^3$ of atmosphere. Fluctuations in the brightness temperature measurements (noise) is limited to less than 0.3K by the 1 second integration time per spot and 200 MHz bandwidth of the channels.

There are about 3000 useful scan lines per day, each including the 11 footprint observations. The MSU LT channel is an effective channel derived by a linear combination of the MSU MT channel at different scan angles. This channel retrieval scheme utilizes only 8 the footprint observations for the scan-line retrieval. Hence, the maximum number of distinct observations on a given day is about 24000 [Christy, *et al.*, 1995].

Once every scan, the instrument makes calibration measurements, viewing deep space (2.7K) and high emissivity warm targets. There is one target for the two lower frequencies, channels 1 and 2, and another for the two highest frequencies, channels 3 and 4. The temperature of each target is monitored with redundant platinum resistance thermometers.

2.2 Weighting Functions

The MSU radiometer senses oxygen emissions at frequencies of 50 to 60GHz. Emissions of electromagnetic radiation through the atmosphere are produced by molecular oscillating dipole charges. The oxygen molecule does not have a permanent electric dipole, but it does possess a permanent magnetic dipole moment as a result of unpaired orbital electrons. The great abundance of the oxygen molecule, relative to the other absorbing molecules, compensates for these weak transitions, ultimately producing a large atmospheric emissions [Stephens, 1994]

At these frequencies radiation emitted by oxygen is proportional to temperature and the blackbody temperature which would emit the same amount of radiation at the given wavelength is referred to as brightness temperature. For the MSU the only time

oxygen is not considered to be an equivalent blackbody is at the earth's surface where the contribution of surface readings and the amount of energy that is being transmitted is going to depend on the surface temperature where the emissivity of less than 1 (grey body). There is a significant difference between land and ocean emissivity, contributing to different values by the MSU sensor. Differences in land types also play an important part in the sensor reading, and, although not investigated in depth in this work, readings from the MSU over the polar regions with ice/snow as the dominate surface may have interpretation errors. Therefore, the surface contribution to the radiance that is sensed will depend on the assumption of a surface emissivity. For the MSU an average over *all* land types emissivity is taken as approximately 1, and for ocean emissivity, 0.5.

The effects of frozen precipitation on MSU sensed energy is a concern. In the MSU's region ice particles must become precipitation size to cause a significant effect [Spencer, *et al.*, 1990]. Empirical evidence for this is shown from the more ice-sensitive 85.5 GHz channel of the Special Sensor Microwave/Imager, which reveals no case of cirrus-induced brightness temperature cooling at the brightness depression level of 0.5°C. If, however, the cirrus are thick and the result of deep moist convection, larger brightness depressions (in excess of 1°C) do occur, which in every case have been linked to evidence of precipitation-sized particles. UAH and RSS groups have used these results as a threshold to eliminate readings that are affected by ice-precipitation size particles.

As electromagnetic radiation propagates through the atmospheric oxygen it is attenuated by absorption seen by [Stephens, 1994]:

$$k_\nu = \frac{S \frac{p}{p_0} \alpha_L}{(\nu - \nu_0)^2 + \alpha_L^2 \left(\frac{p}{p_0} \right)^2} \quad (2.1)$$

where k_ν is the absorption coefficient, S is the strength of the absorption line and a measure of how readily a given oxygen molecule energy state transition takes place. α_L is the line halfwidth, a coefficient that accounts for collisions of the individual molecules in the atmosphere. p is pressure, $p_0 = 1$ atmosphere, ν is frequency and ν_0 is the frequency at line center, and in this case would be ~ 60 GHz

The change in intensity of the radiation as it passes through the atmosphere is given by

$$\frac{dI_\nu}{ds} = -k_\nu I_\nu \rho \quad (2.2)$$

where I_ν is the energy transmitted through the atmosphere, ρ the mixing ratio of oxygen and s is the distance through the atmosphere

Equation 2.2 can be integrated to derive the amount of energy that is transmitted through the atmosphere (τ_ν):

$$\tau_\nu(s_1, s_2) = \exp \left[- \int_{s_1}^{s_2} k_\nu ds \right] \quad (2.3)$$

How τ_ν changes vertically through the atmosphere relates to the contribution from that individual layers sensed by the satellite and is called the weighting function (WF).

$$WF = \frac{d\tau_\nu}{d(*)} \quad (2.4)$$

where (*) is any atmospheric height parameter (e.g., P , $\ln P$, z).

Using these relationships and a known atmospheric profile, the weighting function for MSU channels can be estimated. Figure 2.1 shows the MSU LS and MT weighting functions using the United States Standard Atmosphere vertical profile.

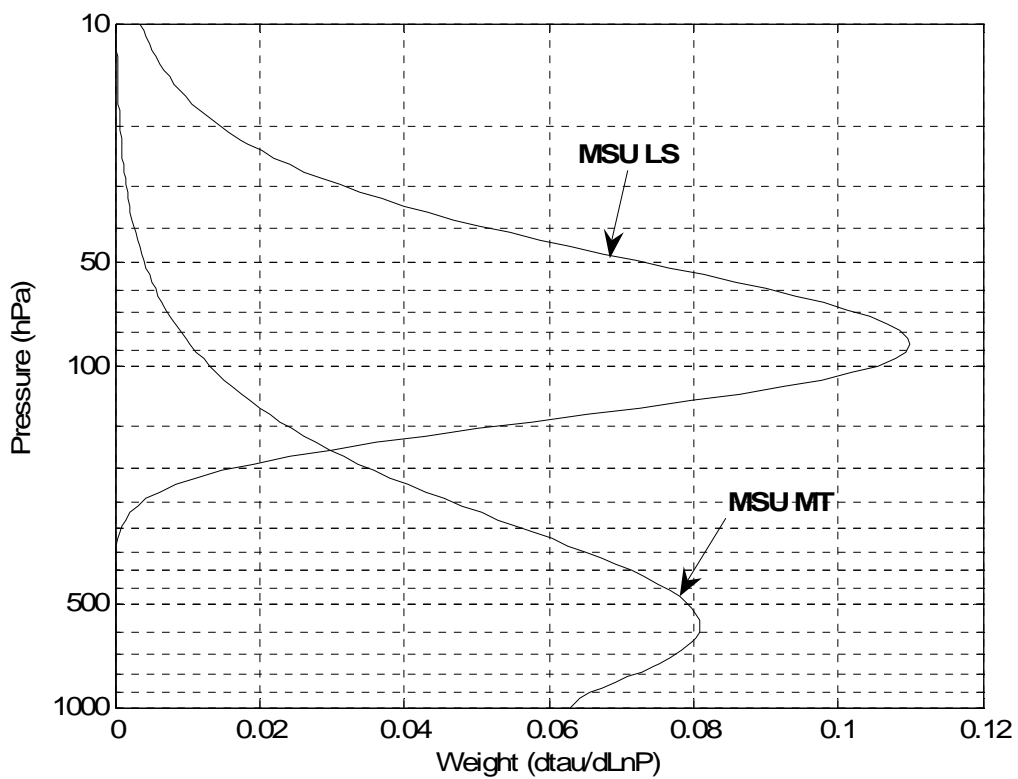


Figure 2.1 Change in transmission of electromagnetic radiation with height creates a weighting function. The weighting function indicates the contribution from a layer in the atmosphere to the overall brightness temperature. Shown here are the MSU LS and MT Weighting functions.

CHAPTER 3

DATA

3.1 Satellite

This work is based on two different MSU data sets. One is produced by Remote Sensing Systems (RSS) and sponsored by the NOAA Climate and Global Change Program. Data are version 3.0 and available at www.remss.com and described in *Mears et al.*, [2003] and *Mears and Wentz*, [2005]. The other is from the University of Alabama at Huntsville (UAH), is available at <http://vortex.nsstc.uah.edu/>, and described in *Christy and Spencer*, [2005] and *Christy et al.*, [2003]. The LT data from UAH are from the updated version (v5.2).

3.2 Radiosonde

Radiosonde data are used independently to compare the two MSU data sets. The radiosonde data used here are based on the temporally homogenized data set described in *Free et al.*, [2005] available at <http://www.ncdc.noaa.gov/oa/cab/ratpac/index.php>. RATPAC-B database which contains monthly anomalies and individual radiosonde sites is used. Only those radiosonde sites and times that were found to be “good” by Randel and Wu [2006] are used, thereby minimizing a long term cooling bias. This tailoring of the RATPAC data enables the radiosonde data to be in excellent agreement (variability and trend) with the MSU LS channel data [*Randel, et al.*, 2007]. From this point forward this tailored RATPAC dataset will be termed RATPAC(RW). A list of the specific sites used in this study is provided in Table 3.1. The radiosonde data are for specific pressure

levels (Sfc, 850hPa, 700hPa, 500hPa, 300hPa, 250hPa, 200hPa, 150hPa, 100hPa, 70hPa, 50hPa and 30hPa).

To compare the radiosonde and MSU satellite data, we integrate the radiosonde temperatures vertically using the LT, MT and LS static weighting functions following procedures in Christy, et al., [2003] (see Figure 2.1).

3.3 Surface

In order to discuss briefly atmospheric amplification (greater warming in the tropopause than the surface) 25-year trends were calculated. The merged land air and sea surface temperature anomaly analysis (Global Historical Climatology Network (GHCN) of land temperatures merged with the Comprehensive Ocean-Atmosphere Data Set (COADS) of SST data) and the HadCRUTv2 created by the Hadley Centre of the UK Met Office were used. Both databases are available at <http://www.ncdc.noaa.gov/gcag/gcag.html>.

3.4 Limited Time Periods

A linear fit over the entire time period to compare long term trends may not be the best technique to compare the databases in order to diagnose differences between derived temperature trends as have been done in the past. Comparing the data over shorter, or limited time periods (LTP), affords the opportunity to determine how methods affect data for the actual time period over which differences in merging methods are used or over time periods used to create coefficients, helping to determine the merits of the methods more accurately. Any similar discrepancies among the methods found at more than one LTP thus could be resolved in a single process used over those time periods. These

similar discrepancies may not be seen using one long term linear trend. Furthermore some changes in climate forcing (e.g., stratospheric ozone, solar radiation, methane) have different trends over time periods shorter than the entire 28-year MSU period. Forcings over LTP may lead to temperature changes in the atmosphere also over LTP, stressing the importance of analyzing the atmosphere over several LTP to understand the complex feedback processes. LTP used in this work are least square linear running trends over 5, 10, 15, 20 and 25-year time periods.

Table 3.1 RATPAC-B database which contains monthly anomalies and individual radiosonde sites is used. Only those radiosonde sites and times that were found to be “good” by Randel and Wu [2006] are used, thereby minimizing a long term cooling bias.

Station	Latitude	Top level (hPa) with continuous data
Amundsen-Scott (00Z)	-90.0	10
McMurdo (00Z)	-77.9	30
Syowa (00Z)	-69.0	20
Macquarie Island (12Z)	-54.5	50
Marion Island (00Z)	-46.8	20
Gough Island (00Z / 12Z)	-40.3	20
Martin de Vivies (12Z)	-37.8	30
Adelaide (12Z)	-34.9	30
Capetown (00Z)	-33.9	20
Durban (00Z)	-29.9	20
Norfolk Island (00Z)	-29.0	20
Rio de Janeiro (12Z)	-22.8	20
Townsville (00Z)	-19.2	20
Darwin (00Z)	-12.4	20
Manaus (12Z)	-3.1	20
Nairobi (00Z)	-1.3	20
Bangkok (00Z)	13.7	30
San Juan (00Z / 12Z)	18.4	10
Hilo (00Z / 12Z)	19.7	10
Jeddah (12Z)	21.6	20
Minamitorishima (12Z)	24.3	20
Brownsville (00Z / 12Z)	25.9	10
Santa Cruz (12Z)	28.4	20
Kagoshima (12Z)	31.6	20
Bet Dagan (00Z)	32.0	50
Miramar (00Z / 12Z)	32.8	10
North Front (00Z / 12Z)	36.2	10
Dodge City (00Z / 12Z)	37.7	10
Kashi (00Z)	39.4	20
Wakkanai (00Z / 12Z)	45.4	20
Rostov (00Z)	47.2	30
Great Falls (00Z)	47.4	10
Torbay (00Z)	47.6	20
Munchen (00Z / 12Z)	48.2	20
Moosonee (00Z / 12Z)	51.2	20
Petropavlovsk (12Z)	53.0	20
Omsk (00Z / 12Z)	54.9	20
Annette Island (00Z)	55.0	10
Saint Paul Island (00Z)	57.1	10
Kirensk (00Z / 12Z)	57.7	30
Lerwick (00Z / 12Z)	60.1	20
Keflavik (00Z / 12Z)	64.0	20
Baker Lake (00Z / 12Z)	64.3	20
Pechora (00Z)	65.1	30
Turuhansk (00Z / 12Z)	65.8	20
Verkhoyansk (00Z)	67.6	30
Alert (12Z)	82.5	10

CHAPTER 4

STATISTICAL METHOD EVALUATION USING LIMITED TIME PERIODS

4.1 Introduction

As can be seen from Figure 4.1, the MT channel weighting function extends above the tropopause and therefore, the resulting channel MT temperature will be influenced to some extent by the stratosphere. Monitoring tropospheric temperature trends from MSU depends conceptually upon the removal of the stratospheric influence from the MSU MT channel [Spencer, *et al.*, 2006] (see Figure 4.1). Fu and Johanson [2004a] (FJWS) proposed a statistical method that relies on interlayer correlations from radiosonde data [Spencer, *et al.*, 2006]. Some studies show the robust nature of this statistical method using computer model simulations [Gillett, *et al.*, 2004; Kiehl, *et al.*, 2005]. A debate continues however as to the accuracy of removing the stratospheric influence on MT using statistical means [Fu and Johanson, 2004b; Spencer, *et al.*, 2006; Tett and Thorne, 2004]. The method was updated to define the resultant temperature trend to be for the entire troposphere, instead of the 850 hPa – 300 hPa layer as in the original work. In addition, computation of coefficients from two different radiosonde datasets was accomplished to show independence of training dataset [Johanson and Fu, 2006] (JF06).

The purpose of this chapter is to investigate the ability of statistical regression techniques, including JF06, to eliminate the stratospheric influence on the MT channel temperature trends using LTP. In doing so the latest radiosonde database available (RATPAC(RW)) is used. In order to assign atmospheric variability to errors found in the statistical determination of a combined MT and LS channel, 15, 20 and 25-year LTP

trends were produced using RATPAC(RW) radiosonde data where the level of zero trend or zero trend level (ZTL) is introduced and further discussed in Section 4.1. The FJ06 method is reviewed in Section 4.2 and the additional regression methods used in this chapter are discussed in Section 4.3. Results and discussion of regression methods are presented in Section 4.4. Other issues associated with using the MT and LS channel combination are discussed in Section 4.5, with summary and conclusions for this chapter in section 4.6.

4.2 RATPAC(RW) Limited Time Period trends / Zero Trend Level (ZTL)

The statistical combination of the MT and LS channels by JF06 did not use the RATPAC(RW) radiosonde dataset. Here 15, 20 and 25-year LTP trends were produced using the JF06 techniques but, with the RATPAC(RW) radiosonde data. Trends are calculated for each radiosonde level over the given LTP using data from January 1958 to December 2006. The 15-year LTP trends are shown in Figure 4.2a for globally averaged data and Figure 4.2b for the tropics (20°N-20°S). Figure 4.3 shows 20-year LTP with the 25-year LTP in Figure 4.4.

Key features to focus on for this paper are the vertical distribution of temperature trends and the level where the trend is zero (ZTL). The vertical distribution of temperature trends indicates mainly warming in the troposphere and strong cooling in the stratosphere. In Figure 4.2a it can be seen that the strongest cooling in the globally averaged stratosphere is over the 15-year trends centered on 1991 through those centered on 1997. In addition, stronger cooling over the 15-year trends centered on 1965 though those centered on 1972 is seen. The periods of strong stratospheric cooling are important

to note because the LS channel encompasses this cooling and is used to eliminate stratospheric contributions when regression methods are applied using the LS and MT channels. Another important metric to consider when dealing with the LS and MT combination is the vertical variability of the ZTL. Figure 4.2a shows the globally averaged ZTL varies anywhere from above 30 hPa (upper limit in radiosonde data) in the 15-year trend centered on 1976 to ~ 300 hPa for 15-year trends centered on the early 1990's. For 20-year globally averaged LTP the ZTL varies over a range of ~80hPa-250hPa (Figure 4.3a), and for the 25-year globally averaged LTP over a range of ~100hPa-200hPa (Figure 4.4a). This region of variability is through the layer where the weighting functions for the LS and MT channel are not equal, but large enough where neither weighting function can be neglected (see Figure 4.1). This then establishes the need to further explore techniques that use a combination of the LS and MT channel.

It is possible that causes of this variability of cooling and warming in the upper troposphere/lower stratosphere may be related to ozone depletion and recovery, water vapor variability or variability in the solar spectral output. However, a comprehensive study into the effects of these parameters over LTP would be necessary to confirm this hypothesis. This and whether the ZTL can be used as a metric for climate studies is left to further study.

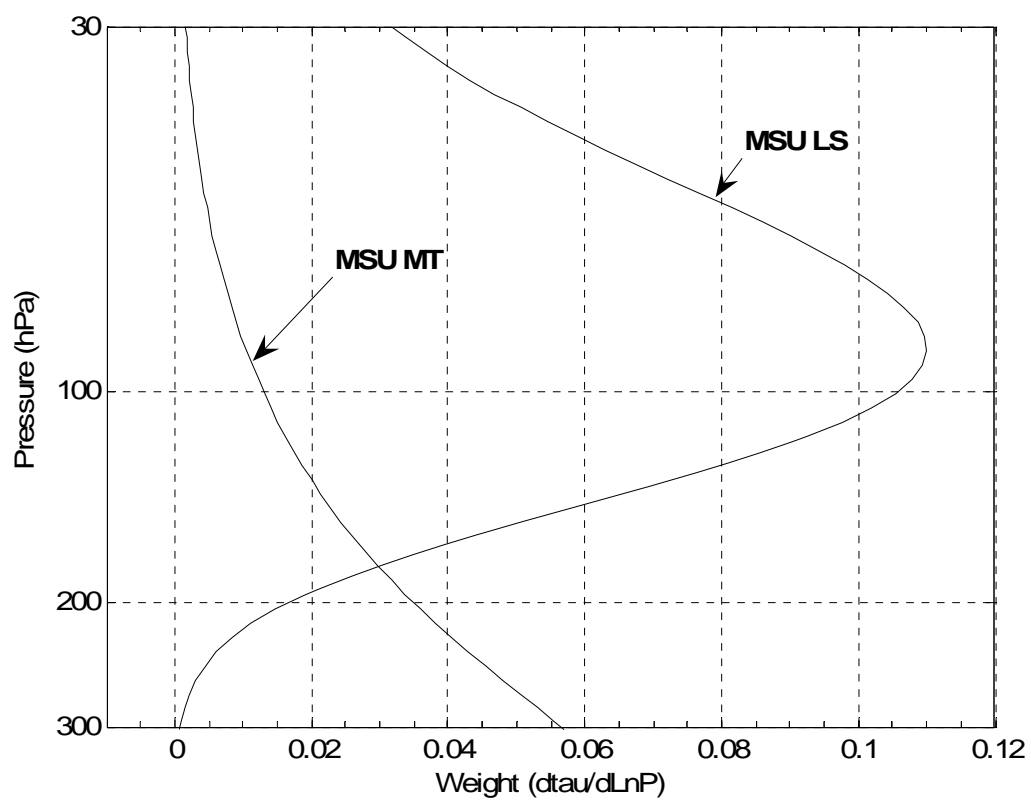


Figure 4.1. Layer where the MSU LS and MT weighting function intersect. The MT channel has a significant contribution from the stratosphere (above 200 hPa for global average). The biggest impact for a combination of the two channels is between 100 hPa and 200 hPa, the region of greatest variability in the ZTL.

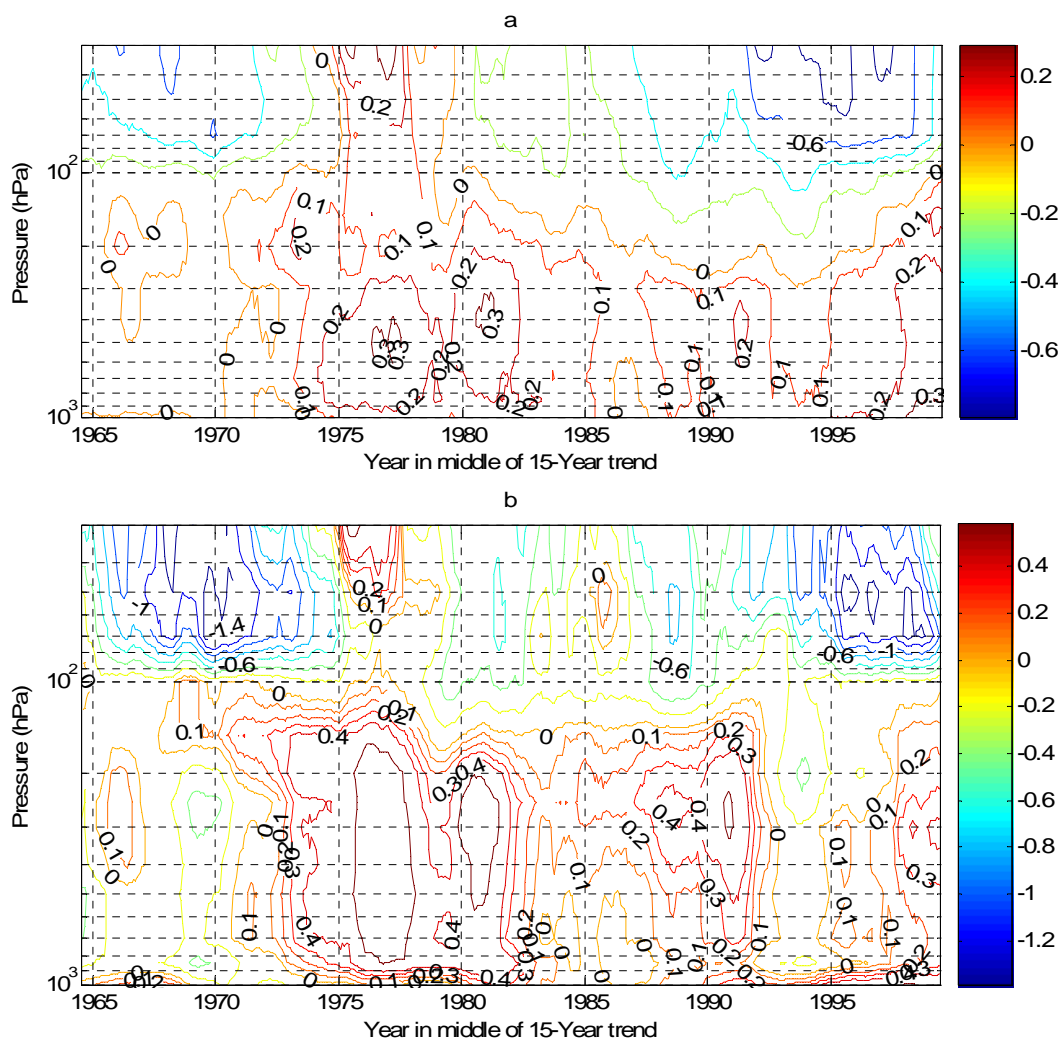


Figure 4.2 (a) 15-year Limited time period trends (K/decade) on globally averaged RATPAC(RW) data. Key features are strong cooling seen in trends centered on 1991 through those centered on 1997 and ZTL variability from 30 hPa to ~300 hPa. (b) Tropical (20°N - 20°S).

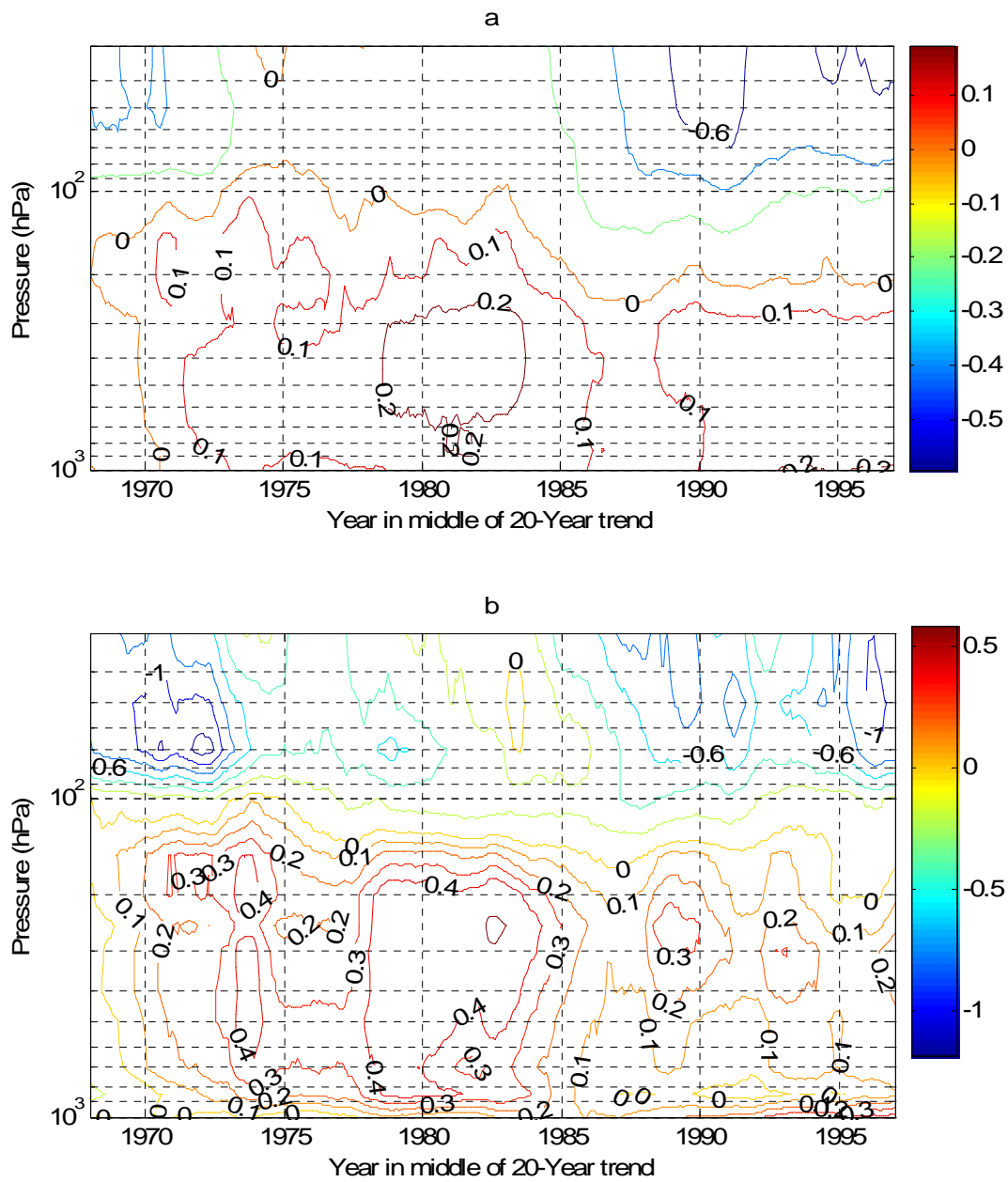


Figure 4.3 Same as Figure 4.2 for 20-year LTP (K/decade).

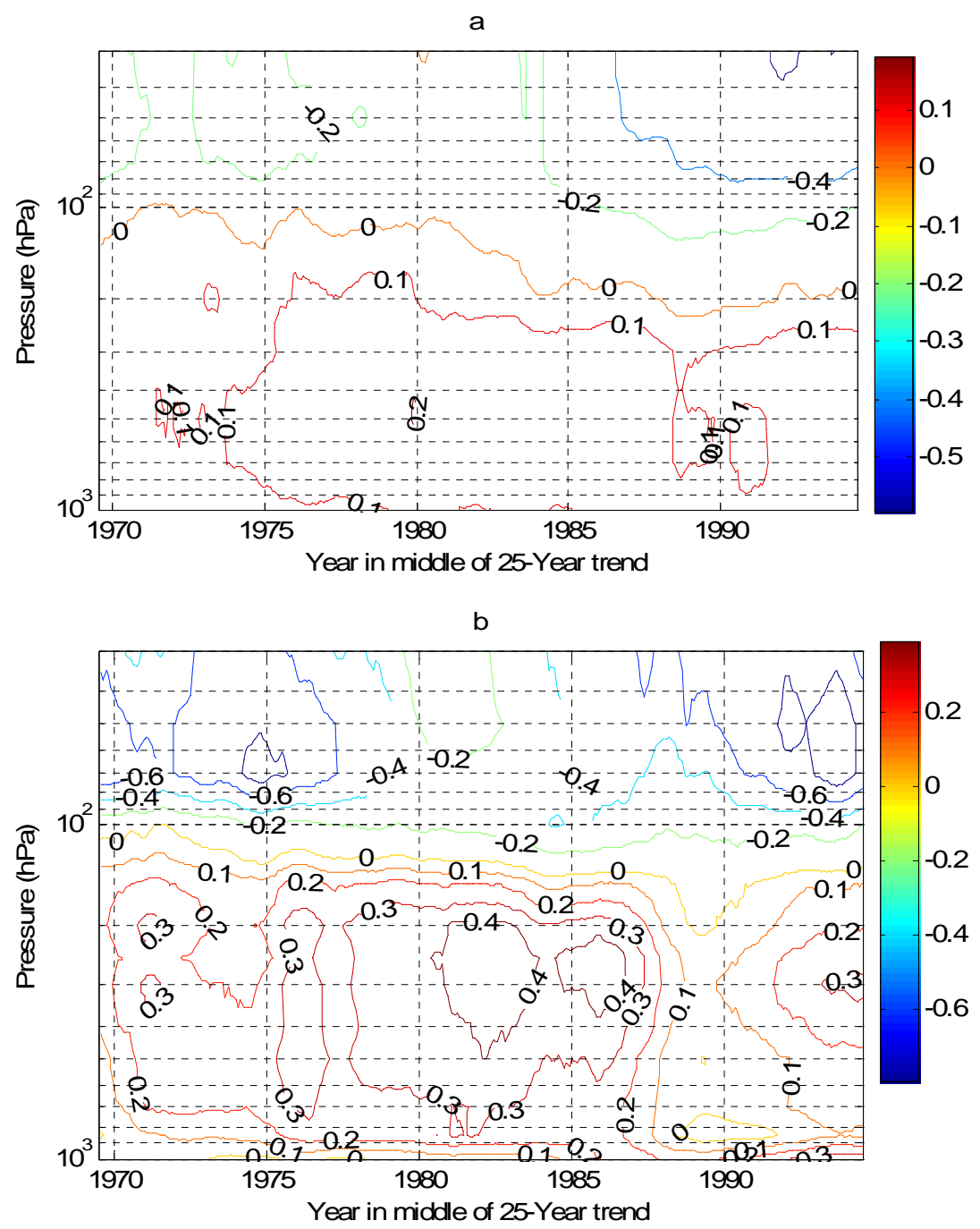


Figure 4.4 Same as Figure 4.2 for 25-year LTP (K/decade).

4.3 Review of JF06 regression method

As seen in Figure 4.1, the MT channel weighting function extends well into the stratosphere. FJWS created a method to eliminate the stratospheric influence from the MSU MT channel in order to get a more accurate estimate of tropospheric only temperature change. Their original method was subsequently modified and is explained in JF06. In order to estimate the tropospheric temperature from the MT and LS channels, JF06 used the form

$$T_{TR} = a_0 + a_{MT}T_{MT} + a_{LS}T_{LS} + \varepsilon, \quad (4.1)$$

where T_{TR} is the estimated tropospheric temperature, T_{MT} and T_{LS} are the MT and LS temperatures respectively and ε is the error. The regression coefficients a_{MT} and a_{LS} are computed from a linear least squares fit, minimizing ε^2 , using simulated MT and LS channel monthly average temperature anomalies using radiosonde data and a tropospheric layer temperature (T_{TR}) calculated from radiosonde data in the form

$$T_{TR} = \frac{W_s T_s + \int_{1000}^{P_t} W_{MT}(p) T(p) dp}{W_s + \int_{1000}^{P_t} W_{MT}(p) dp}. \quad (4.2)$$

Note that T_{TR} computed in this manner represents the temperature that would be measured with the MT channel weighing function through the layer from 1000 hPa to P_t . W_{MT} is the T_{MT} weighting function, W_s is the relative contribution of the surface temperature (T_s), $T(p)$ is the atmospheric temperature profile, and P_t is the tropopause pressure. P_t is 200 hPa for the global mean and 100 hPa for the Tropics taken to be 20°S-20°N in this work. (Note that JF06 used 30°S-30°N for the tropics)

To compute the simulated MSU values for T_{MT} and T_{LS} for Equation 4.1 the radiosonde temperatures are vertically integrated using the MT and LS static weighting functions following procedures in Christy et al., [2003]. The a_0 is very small and not necessary for trend analysis and is therefore not considered. In addition, the trends for T_{TR} , T_{MT} , and T_{LS} are removed prior to regression and JF06 used $a_{MT} = 1 - a_{LS}$ as an additional constraint as a means to create a normalized effective weighting function, discussed further in section 4.4.

4.4 Methods of regression using LTP analysis

In order to assess all of the regression methods for LTP trends, coefficients for all the methods are computed from RATPAC(RW) using least squares regression methods in various ways. T_{TR} is then derived from equation (4.1) using the coefficients derived from these various methods and compared to the actual T_{TR} computed from equation (4.2). The various methods used for creating coefficients using least squares regression follow.

4.4.1 RH07

This technique was developed as an alternative method to eliminate effects on T_{MT} of the stratosphere above the top of the required level. Regression coefficients are calculated using only the MT static weighting function as opposed to all other methods which use a combination of the MT and LS channel. The same process as JF06 was produced except only the MT channel was used. T_{TR} remained the same, however the actual stratospheric contribution to the MT channel is:

$$T_{MT(ATROP)} = \frac{\int_{P_i}^0 W_{MT}(p)T(p)dp}{\int_{P_i}^0 W_{MT}(p)dp}, \quad (4.3)$$

where $T_{MT(ATROP)}$ is the weighted temperature of the MT channel above the P_i level.

Coefficients were found using the MT channel, $T_{MT(ATROP)}$ and T_{TR} as the target layer and are termed RH07 (see Figure 4.5a). This creates a linear regression from two physical layers, each weighted by MT and is therefore, an exact fit to the MT channel.

Coefficients for $(a_{MT(ATROP)}, a_{MT})$ are $(-0.167, 1.167)$, using the RATPAC(RW) radiosonde temperatures.

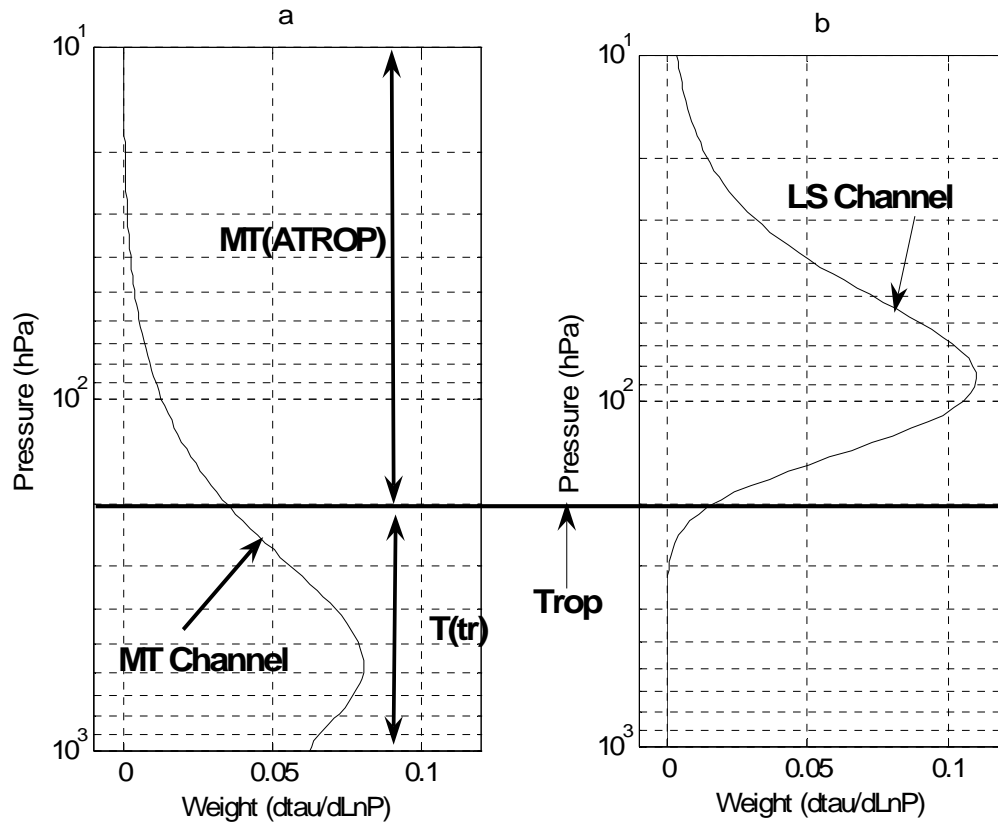


Figure 4.5 (a) MT weighting function. RH07 subtracts the layer above the tropopause (MT(ATROP)) from the entire MT channel to estimate the tropospheric layer (T_{TR}). (b) LS weighting function. Methods other than RH07 use the LS and MT channels to estimate the tropospheric layer (T_{TR}).

Note that the constraint of $a_{MT} = 1 - a_{LS}$ was not imposed on the RH07 coefficients, they are the actual coefficients calculated. They sum to 1 because $T_{MT(ATROP)}$ and T_{TR} are the actual weights of MT channel for their respective layers and the MT channel has been already normalized to 1. This regression method was run on all LTP and the variation in coefficients was < 0.0001 ; essentially constant, as one would expect.

4.4.2 JF06NEW

Next, the FJ06 method was used to calculate coefficients from the RATPAC(RW) radiosonde dataset. Coefficients were calculated using the full 1958-2006 time period and were found to be ($a_{LS} = -0.0977$, $a_{MT} = 1.0977$), using the constraint $a_{MT} = 1 - a_{LS}$. These constant coefficients were then used on each LTP to estimate T_{TR} (termed JF06NEW). Coefficients were also calculated for each individual 15, 20 and 25-year LTP and then each individually derived set of coefficients were applied to its corresponding LTP to estimate T_{TR} (termed JF06NEWXX where XX is the LTP used). FJ06 used the constraint $a_{MT} = 1 - a_{LS}$. As discussed below however this is not physically sound and using $a_{LS} = 1 - a_{MT}$ would be an equally valid solution to parameters summing to 1 if constraint is applied after regression is complete, but yield different results. Therefore coefficients are also found using this latter constraint (cs) (termed JF06NEWXXcs) to show the differences.

4.4.3 NoCONST

Actual coefficients for both a_{TM} and a_{LS} were also found from regression to be (-0.0977, 1.119). In other words, the $a_{TM} = 1 - a_{LS}$ constraint was not applied. Coefficients

were calculated using the full 1958-2006 time period of the RATPAC(RW) data. These constant coefficients were then used on each LTP to estimate T_{TR} (termed NoCONST for no constraint used). Coefficients were also found for each individual 15, 20 and 25-year LTP. These individually derived coefficients were applied to their corresponding LTP to estimate T_{TR} (termed NoCONSTXX; where XX is the LTP used).

One must be careful when applying a constraint to sum regression derived coefficients to 1. The true coefficients do not necessarily add up to 1 and to force them to do so is not physically sound or statistically optimal. This can be seen by solving for a_{MT} using equation (4.3)

$$a_{MT} = \frac{T_{TR} - a_{LS}T_{LS}}{T_{MT}} . \quad (4.3)$$

If constraints are applied after regression is complete $a_{TM} = 1 - a_{LS}$ would only be true if $T_{TR} = T_{MT} = T_{LS}$. Actual derived coefficients (NoCONSTXX) and their sum are shown in Figures 4.6 thru 4.8 for 15 thru 25-year LTP's respectively. There are no time periods where the coefficients sum to 1. Thus, selecting a_{MT} to calculate a_{LS} or a_{LS} to calculate a_{MT} becomes a decision that impacts the physical meaning of the coefficients. Using Figure 4.6 as an example, the actual a_{MT} coefficient has a greater variability than the a_{LS} coefficient and seems to follow the variability in magnitude of cooling in the stratosphere (compare with Figure 4.2a), while the a_{LS} coefficient appears to follow ZTL variability in the atmosphere (Figure 4.2a). Whether the constraint is applied before or after regression is complete the resulting normalized coefficients are no longer the best fit to the actual estimated tropospheric temperature. The unconstrained coefficients found from the

regression method are the best fit solution to estimating the tropospheric temperature and should be used.

The JF06 method uses the MT and LS channels so the coefficients derived can be used on the current MSU data to estimate T_{TR} temperature trends. In an attempt to assess errors created by using regression coefficients using the LS and MT channels when applied to actual MSU data, all aforementioned coefficients were applied to RSS and UAH MSU derived databases to compare results. Note that the physically sound regression coefficients derived from RH07 do not use the MSU LS channel. The UAH data however closely follow the radiosonde temperature data weighted with the MT weighting function. An estimated T_{TR} can therefore be found by applying the coefficients derived in this manner using the $T_{MT(ATROP)}$ found from the radiosonde and UAH MT channel. Additionally we used the coefficients found in the actual JF06 for globally averaged data (-0.141, 1.141) (termed JF06OLD). Table 4.1 summarizes the methods for calculating coefficients.

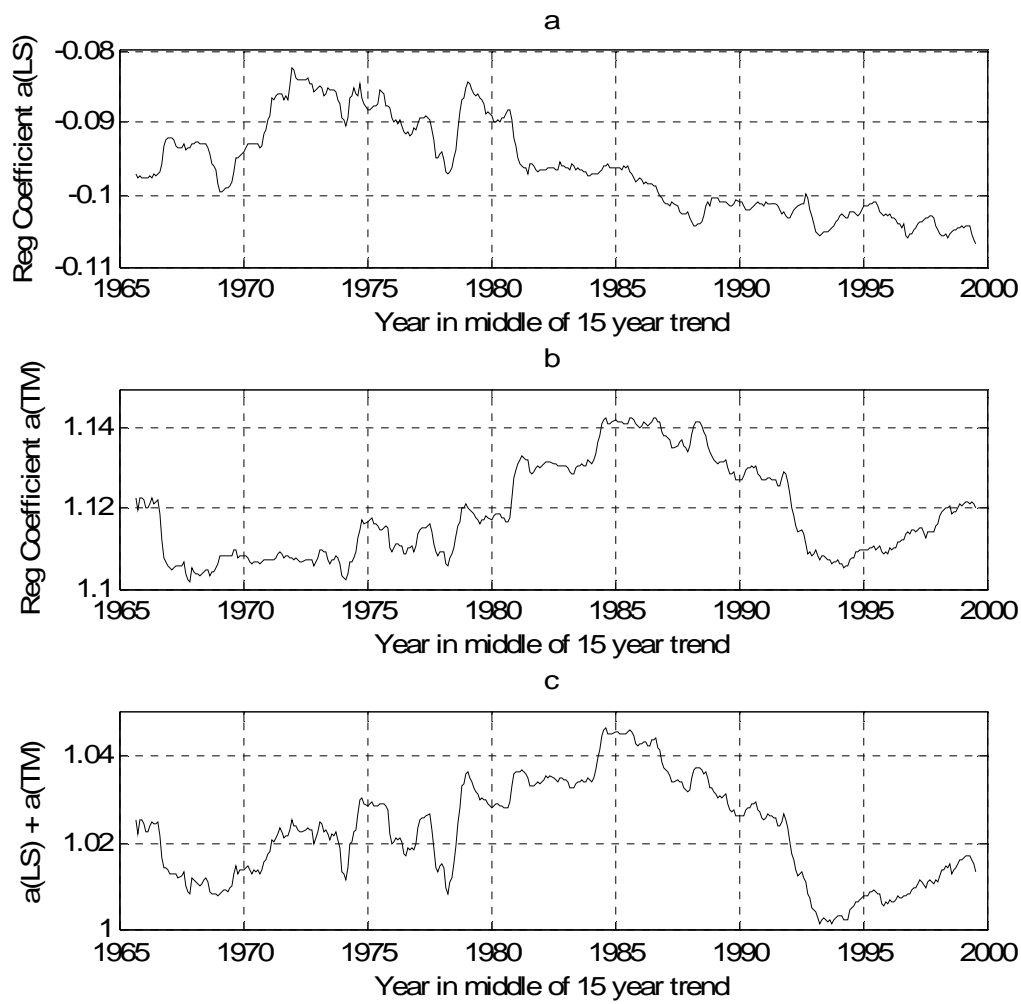


Figure 4.6 (a) $a(\text{LS})$ coefficient found using least squares regression at each 15-year LTP. (b) same as (a) for $a(\text{TM})$ coefficient. (c) $a(\text{LS}) + a(\text{TM})$. There are no time periods where the actual coefficients sum to 1 as constrained by FJ06. Forcing them to do so no longer give the coefficients that provide the best fit to the estimated tropospheric temperature.

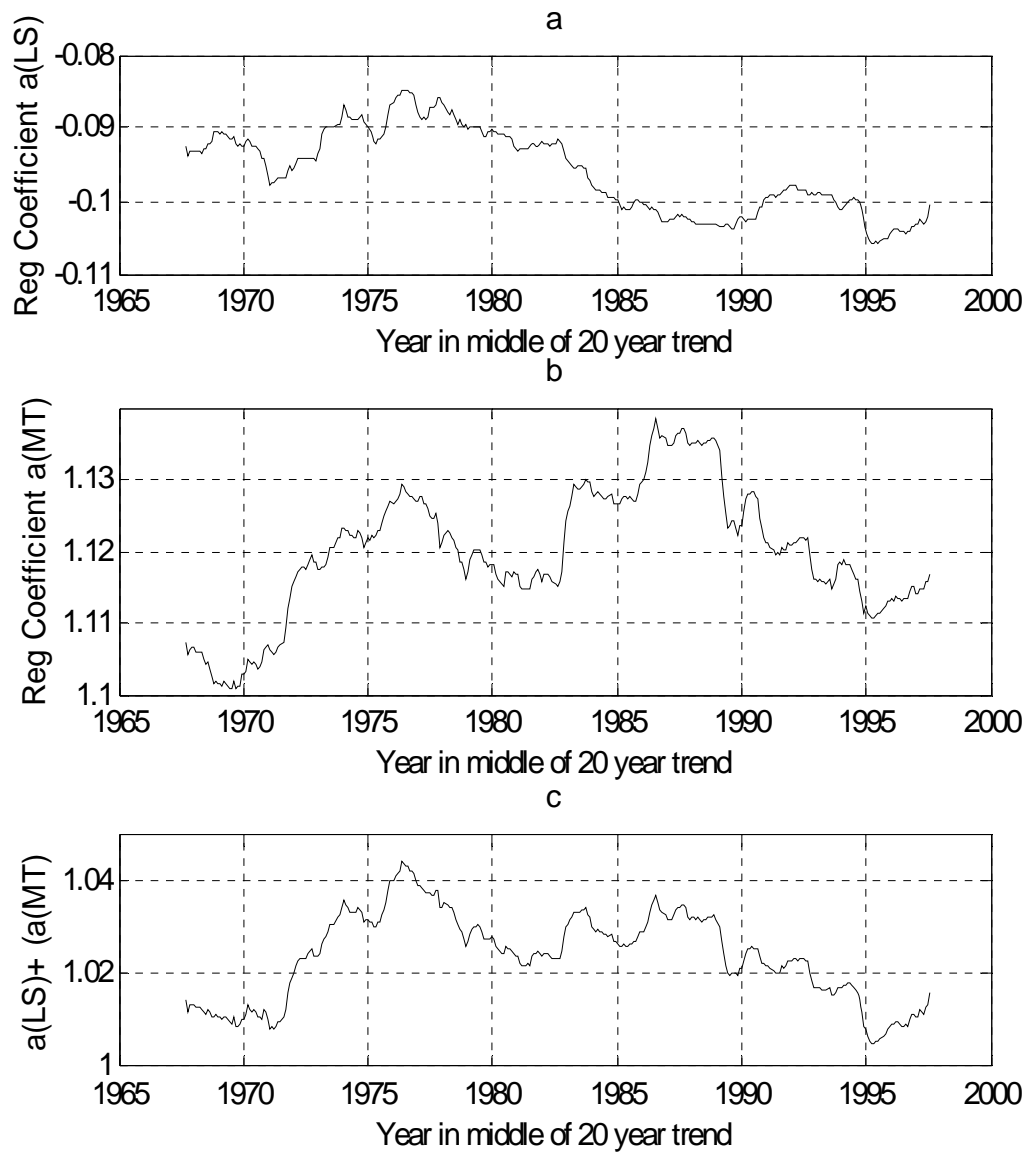


Figure 4.7 Same as Figure 4.6 for 20-year LTP

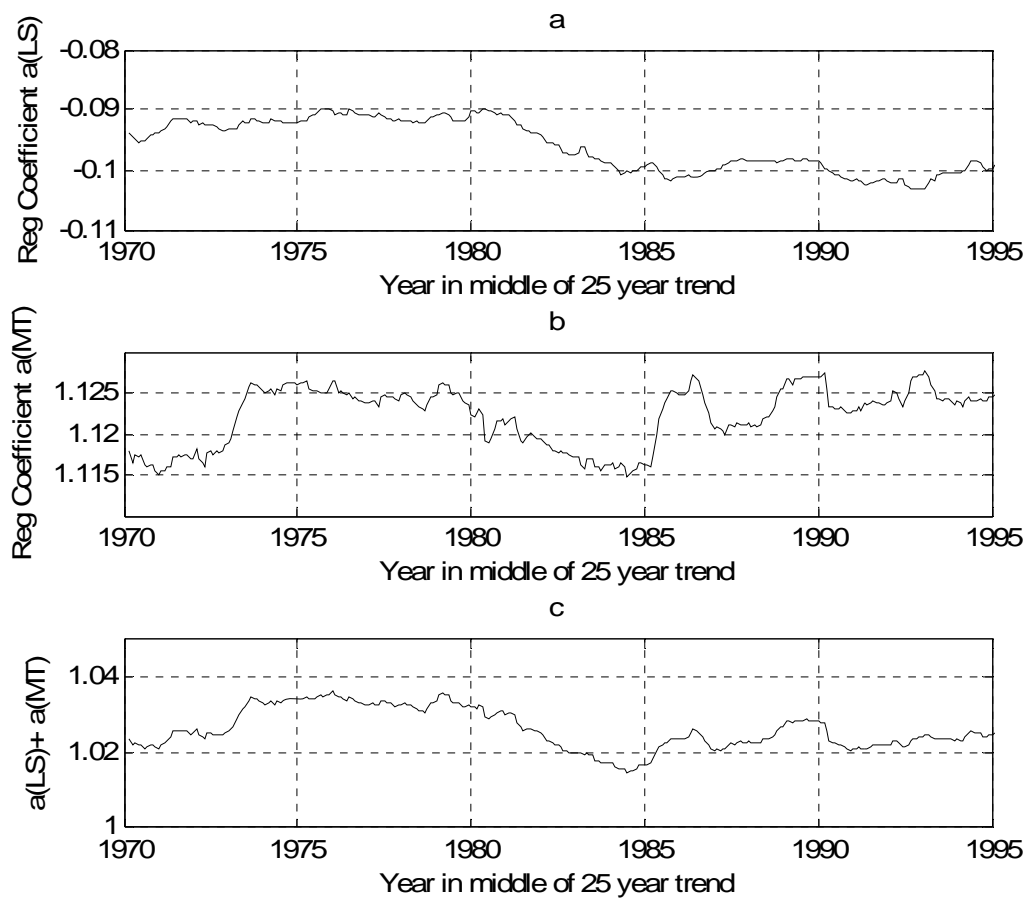


Figure 4.8 Same as Figure 4.6 for 25-year LTP

Table 4.1 Techniques used to calculate globally averaged regression coefficients

Name	(a_{LS}, a_{MT})	Derivation technique
<i>RH07</i>	<i>(-0.067, 1.067)</i> <i>($a_{MT(ATROP)}$, a_{MT})</i>	<i>Physical separation of MT Channel</i>
<i>JF06NEW</i>	<i>(-0.098, 1.098)</i>	<i>JF06 method applied to RATPAC(RW)</i> <i>For entire 1958-2006 time period.</i> <i>Constraint: $a_{MT} = 1 - a_{LS}$</i>
<i>JF06NEWXX</i>	<i>See Figures:</i> <i>4.6a-4.8a</i>	<i>JF06 method applied to RATPAC(RW)</i> <i>for each LTP. Constraint:</i> <i>$a_{MT} = 1 - a_{LS}$</i>
<i>JF06NEWXXcs</i>	<i>See Figures:</i> <i>4.6b-4.8b</i>	<i>JF06 method applied to RATPAC(RW)</i> <i>for each LTP. Except constraint:</i> <i>$a_{LS} = 1 - a_{MT}$</i>
<i>NoCONST</i>	<i>(-0.098, 1.119)</i>	<i>Actual coefficients from RATPAC(RW)</i> <i>For entire 1958-2006 time period.</i> <i>No constraint applied</i>
<i>NoCONSTXX</i>	<i>See Figures</i> <i>4.6(a,b)-4.8(a,b)</i>	<i>Actual coefficients from RATPAC(RW)</i> <i>for each LTP. No constraints applied</i>
<i>JF06OLD</i>	<i>(-0.141, 1.141)</i>	<i>From Johanson and Fu [2006]</i>

4.5 Results of regression methods using LTP

All methods of creating coefficients, except JF06OLD, were applied to 15,20 and 25-year LTP from RATPAC(RW) radiosonde data and corresponding T_{TR} were created using equation 4.1. In addition T_{TR} was found using equation 4.2. To see how well the statistical regression methods predict T_{TR} , T_{TR} derived from equation 4.2 were subtracted from those derived by equation 4.1. If the statistical method predicted the target layer trends then this difference would be zero. Differences in trends are shown in Figure 4.9 for 15-year LTP, Figure 4.10 for 20-year LTP and Figure 4.11 for 25-year LTP. The best statistical solution for an LS/MT combination is the NoCONSTXX as this method uses the actual, non-normalized regression coefficients. The first thing to note is that constant coefficients (NoCONST and JF06NEW) have a cooling bias during some time periods and warming bias during others when compared to coefficients calculated at each LTP (NoCONSTXX and JF06NEWXX). During the MSU era it is solely a cooling bias. This is caused by the coefficients being greater than the average during this time frame, which contributes to more warming added back into the trend from the LS channel and more warming accounted for from the greater MT channel coefficient. This can be seen in Figure 4.11a. Here it is seen that 25-year trends prior to those centered on 1984 show a warming bias in constant coefficients (NoCONST and JF06NEW) and trends after those centered on 1984 show a cooling bias in constant coefficient derived T_{TR} . However, it is important to note that while using coefficients created for every LTP is a more accurate

solution, the biases created from using constant coefficients are never greater than 0.005 K/decade (with this database) and would not change the outcome of any T_{TR} study.

Next thing to note is that the JF06NEW T_{TR} has a cooling bias when compared to the NoCONST time series in most LTP. This is due to the constraint that is applied by JF06, where $a_{MT} = 1 - a_{LS}$. The actual a_{MT} is greater than the constrained a_{MT} , which would cause the estimated T_{TR} to have additional warming added from the increased coefficient for the MT channel, increasing the estimated tropospheric temperature trend. One exception to JF06NEW having a cooling bias is when the MT channel is actually cooling. Under this scenario the actual coefficient for the MT channel increases (when compared to JF06NEW) and increases the cooling, this leads to JF06NEW producing a warming bias and is seen in Figure 4.9a in the 15-year LTP trends centered on 1965 through trends centered on 1972. It is also apparent in 20-year LTP trends centered in 1968 through trends centered in 1970 (Figure 4.10a). These time periods can be seen in Figure 4.6 and Figure 4.7 (15, 20-year LTP for RATPAC(RW)) where it is seen that the troposphere has no trend or a slight cooling.

It can also be seen in Figures 4.9a-4.11a that deriving T_{TR} using JF06NEWXXXcs coefficients produces a substantial warming bias over the majority of the time periods and all of the time periods in the MSU era (Figures 4.9b-4.11b). As discussed previously this is a valid solution when constraining the sum of the coefficients to 1 after regression is complete. These results indicate that actual coefficients (NoCONST, NoCONSTXX) should be used if using a combination of the LS and MT channels and constraints are not valid for regression obtained coefficients.

Additionally, RH07 coefficients were also used to estimate T_{TR} (equation 4.1) and subtracted from the actual T_{TR} (equation 4.2), but in each LTP the difference of trends was zero, as expected.

Although there are differences in estimating T_{TR} between each regression method used to calculate coefficients using the MT and LS channels, the differences are < 0.01 K/decade. It is found that the greater differences are between T_{TR} found using *any* LS/MT combination method and the T_{TR} derived from equation 4.2.

It has been shown that differences between the different methods used to create coefficients (using the MT and LS channels) are very small outside of the JF06NEWXXcs, which was provided to show magnitude of error using the constraint $a_{LS} = 1 - a_{MT}$. Any combination of MT and LS (other than JF06NEWXXcs) to estimate T_{TR} however shows time periods where, compared to the actual T_{tr} , errors are as great as 0.02 K/decade (Figure 4.9a) in the 15-year LTP and in 20-year LTP 0.015 K/decade (Figure 4.10a). This leads to errors in trends, in some time periods of greater than 50%. Greatest differences are seen during time periods when the LS channel does not represent the MT channel layer above the tropopause (MT(ATROP)). A good metric to see this is the ZTL discussed in section 4.1. As the ZTL moves upward through the layer above the tropopause (see Figure 4.1) the actual amount of cooling influencing the MT channel becomes less, thus less warming needs to be added back to estimate the tropospheric temperature trend. When strong cooling exists in the layer above the ZTL however the change in the cooling the LS channel can sense, as warming enters the LS weighting function, is small. This is because the amount of warming entering the LS weighting

function is an order of magnitude less than the strong cooling in the stratosphere. In the regression models using MT/LS combinations the LS channel is representing the influence that needs to be eliminated. In the above scenario the LS trend will remain close to the same as it was when the ZTL was below the tropopause, but the cooling that actually needs to be eliminated (MT(ATROP)) will decrease. This causes the LS coefficient to be larger than it needs to be and results in adding back more warming, creating a warming bias in the estimated tropospheric temperature trends. Under these conditions (strong cooling in stratosphere, ZTL above the tropopause) the LS channel does not physically represent the MT influence that needs to be eliminated. The best examples are seen in 15-year LTP trends (Figure 4.9a) centered on 1966 through trends centered on 1974, compared to the atmosphere LTP Figure 4.2a, and the 20-year LTP (Figure 4.10a) from trends centered on 1968 through trends centered on 1972, compared to the atmosphere LTP Figure 4.3a. During these time periods strong cooling exists in the stratosphere and the ZTL is well above the 200hPa tropopause. The 25-year LTP (Figure 4.4a) shows differences between the different time periods when there is cooling in the stratosphere and the ZTL is above the tropopause. However, in the above time period the cooling is not as strong as seen in the 15 and 20-year LTP. Lesser cooling results in errors smaller than 0.01 K/decade for trends 25-years and greater, as JF06 concludes, but translates to relative uncertainty of $> 50\%$ for some 25-year time periods.

As for the MSU era, it is important to note that errors using the radiosonde data are starting to increase in the 15-year trends (see Figure 4.9b). This increase coincides

with a ZTL rise in the last few 15-year LTP trends (Figure 4.2a) and is coincident with strong cooling in the stratosphere.

These results are for the analyzed global averages. There may be, however other situations when other latitudinally averaged temperature trends are analyzed that may show strong cooling/warming in the stratosphere and the ZTL above the chosen tropopause. These are situations where misrepresentation of tropospheric temperature trends would exist.

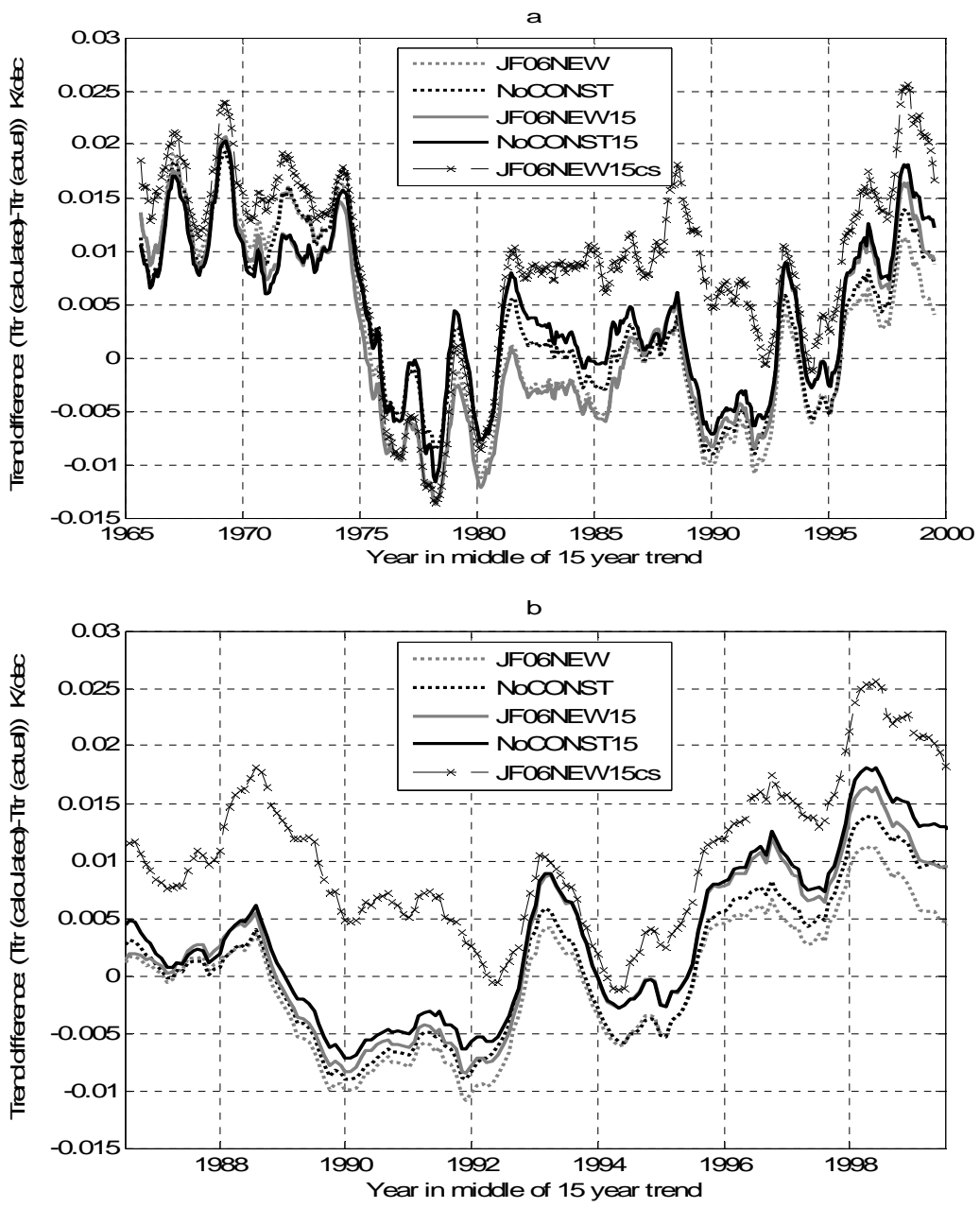


Figure 4.9 (a) Various methods of creating coefficients from RATPAC(RW) radiosonde data and corresponding T_{TR} were created using equation (4.1). These were subtracted from the actual T_{TR} found using equation (4.2) for 15-year LTP over the entire radiosonde time period. (b) Over the MSU era. Any combination of MT and LS (other than JF06NEWXXcs) to estimate T_{TR} shows time periods where, compared to the actual T_{tr} , errors are as great as 0.02 K/decade. These time periods are coincident with strong cooling in the stratosphere and the ZTL above the tropopause.

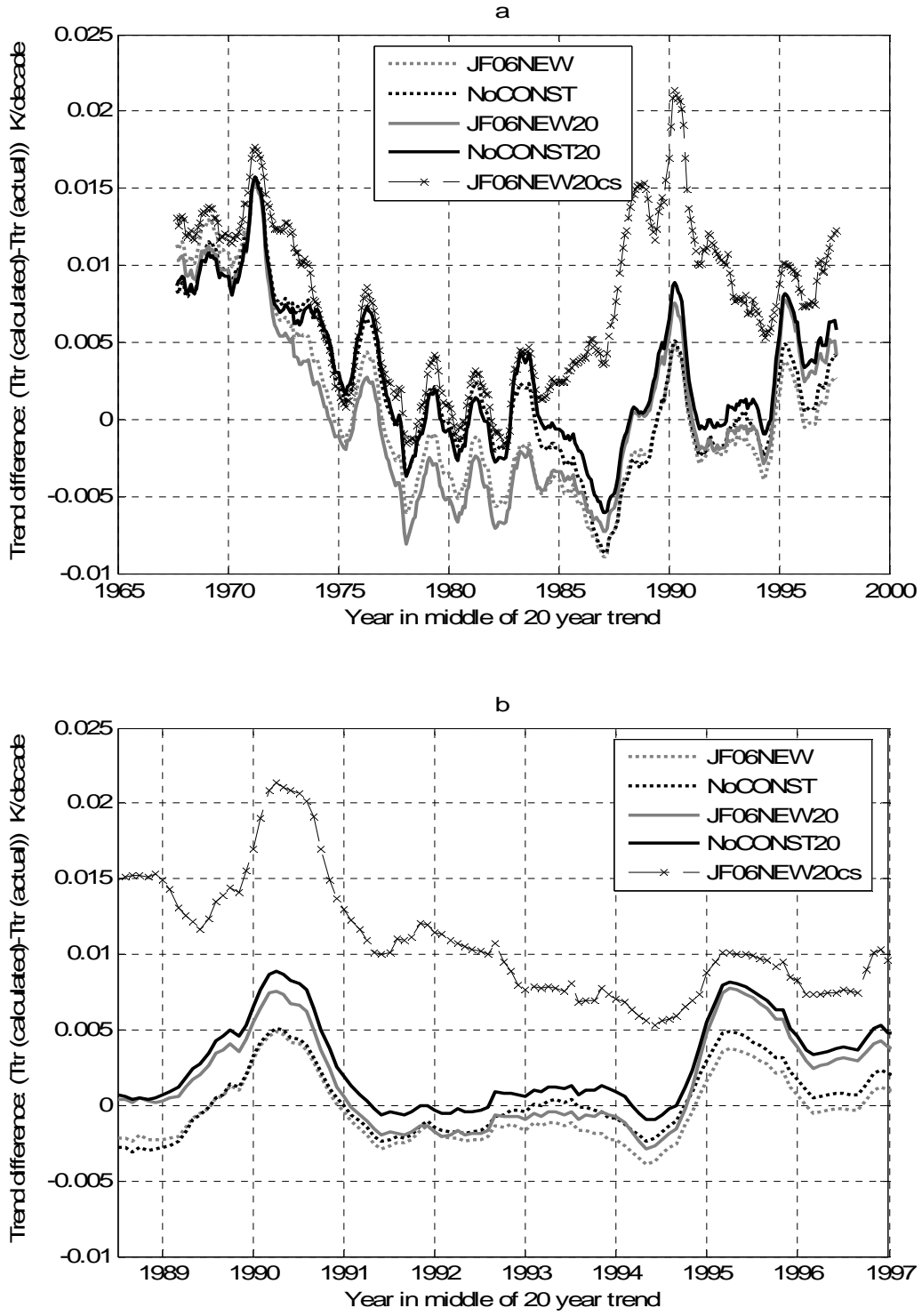


Figure 4.10 Same as Figure 4.9 with 20-year LTP

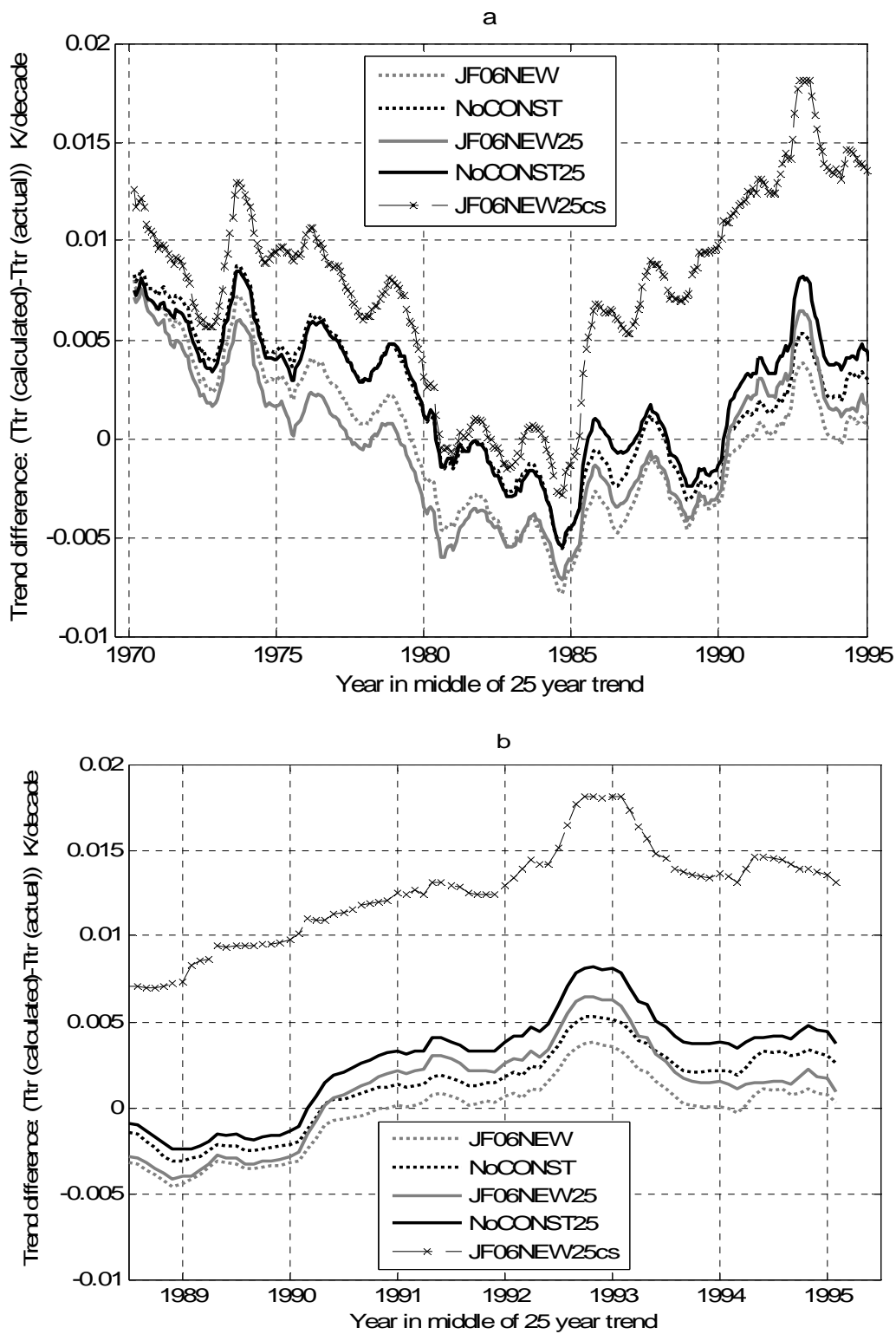


Figure 4.11 Same as Figure 4.9 with 25-year time periods.

To see how the coefficients affect the actual MSU data is a more difficult issue. Previously we compared estimated tropospheric temperature trends created from statistical combinations of the MT and LS channels (equation 4.1) using radiosonde data to compute the coefficients, to the actual tropospheric trends (equation 4.2). When using the actual MSU data, the comparisons of estimated tropospheric temperature trends created from different methods of combining the MT and LS channel can be compared to each other, but an actual tropospheric temperature is not available from MSU data to be the standard. The actual LT channel could be used, but the differences in weighting functions cause the effective height of the resulting temperature to vary, making comparisons difficult. To alleviate this problem the RH07 method was used, combining the UAH MT channel and the MT(ATROP) channel found from the radiosonde data. This is possible with the UAH database because the UAH data closely follow the radiosonde data. The magnitude of the cooling depends on the training dataset used, but the coefficients calculated for (RH07) will not change. Figure 4.12 shows differences of trends which used a statistical combination between MT and LS (computed from UAH data only) and the RH07 method using UAH MT channel and the MT(ATROP) channel found from radiosonde data. Thus this Figure shows: other methods - RH07. The JF06OLD was also included to see how this updated radiosonde data compares to trends found with previously used radiosonde datasets.

Figure 4.12 shows variability consistent with those found in using only radiosonde data. Differences between statistical combinations of the MT and LS channels are within 0.01 K/decade of each other, except JF06OLD. Differences between

JF06OLD and other statistical MT/LS combinations are due to the difference in the dataset used. Although JF06OLD used the RATPAC dataset, the version used with all other methods in this work had those radiosonde sites with cooling biases removed [Randel and Wu, 2006]. Cooling biases in the stratosphere/upper troposphere would cause greater regression coefficients as the coefficient for MT would remain close to constant but the greater LS coefficient would result in adding back more warming, resulting in a greater estimated troposphere temperature. This additional warming indicates using any combination of the MT and LS channels is training database dependent.

Differences between all estimated tropospheric temperature trends using MT/LS statistical combinations and the RH07 method using UAH MT channel and MT(ATROP) from the radiosonde data also show the same error trend as those found when only radiosonde data were used. A trend toward greater errors in 15-year LTP trends centered in the late 1990's is apparent (Figure 4.12), coincident with a signature representative of strong cooling in the stratosphere and a ZTL increasing in height from 300mb to ~100mb (Figure 4.2). Error signatures similar to those found when using only radiosonde data indicate that using UAH data combined with radiosonde data is a good method to indicate estimated tropospheric temperatures with MSU data.

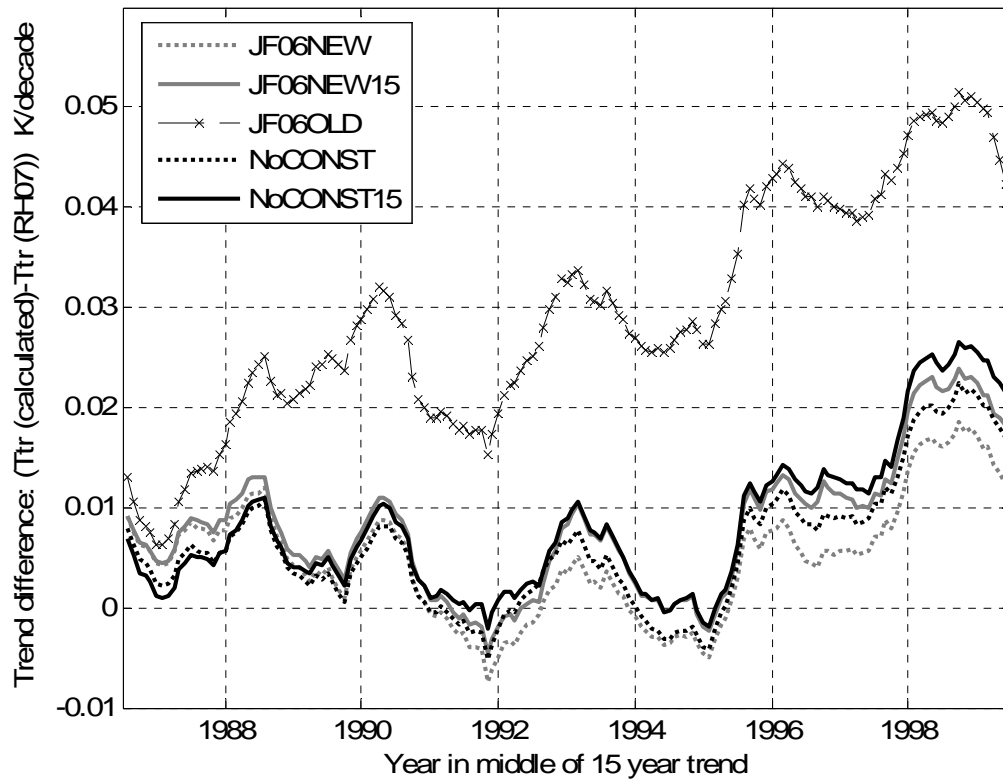


Figure 4.12. Various methods of creating coefficients, were applied to 15-year LTP trends from RATPAC(RW) radiosonde data and corresponding T_{TR} were created using equation (4.1). These were subtracted from T_{TR} found using RH07 and the difference of trends is shown. Differences show the same error trend as those found when only radiosonde data were used. A trend toward greater errors in trends centered in the late 1990's is apparent, these are coincident with strong cooling in the stratosphere and the ZTL above the tropopause.

4.6 Additional issues with using MT and LS combination

4.6.1 MSU instrumentation

As will be shown in the next chapter, methods for merging the MSU data from the various satellites to create a time series contain errors. Most errors are due to correction methods made for diurnal drift in the orbit of each satellite and biases between individual satellites. These problems exist and are different between the LS and MT channels [*Spencer and Christy, 1993*]. Statistical combinations using LS/MT combinations will only magnify any errors that exist in the database, in fact errors in the MT channel are occasionally as large as the trend itself. How these construction or structural errors translate into estimated tropospheric temperature trends will need further investigation.

4.6.2 Static weighting function

The question has been explored as to whether the MSU static weighting function is the best way to estimate temperature trends when simulating MSU temperatures from the radiosonde data. To briefly explore the sensitivity to temperature change when using static weighting functions, the brightness temperature was calculated from a standard atmospheric vertical profile using a static weighting function. A temperature perturbation was imposed on the LS channel using the strongest cooling in stratospheric temperature found in LTP (-1.6 K/decade). Two resulting brightness temperatures were calculated. The first was found by keeping the weighting function constant. The second was found by creating a new weighting function using a radiation

transfer model [Liebe, *et al.*, 1977; Liebe, *et al.*, 1992] and calculating the new brightness temperature. With the above magnitude of cooling in the stratosphere there was only a ~ 0.01 K/decade change in trend between using a static weighing function and using the quasi-dynamic weighting function. This is only 10% of the trend in this region, which translates in a difference in estimated tropospheric trends of ~ 0.001 K/decade, which would be negligible.

4.7 Summary and Conclusions

In this chapter statistical combination of the LS/MT channel, including JF06, using LTP analysis was assessed. In order to do so LTP was accomplished using RATPAC(RW) data and it was found that the ZTL is most variable thru the layer where the combination of the weighing function for the MT and LS channel influenced the estimated tropospheric temperature the most.

Constraining coefficients are not physically sound or statistically optimal and cause errors; therefore, the best method for a MT/LS statistical combination uses actual coefficients derived from the regression method (NoCONSTXX). Using $a_{MT} = 1 - a_{LS}$ as a constraint, after regression is complete, causes a small cooling bias in this radiosonde dataset and using $a_{LS} = 1 - a_{MT}$ causes a large warming bias in the estimated tropospheric temperature. When coefficients are created by regression methods “normalizing” will create coefficients that no longer predict the intended tropospheric temperature trend.

It is found that the greater errors are between T_{TR} found using *any* LS/MT combination method and the actual T_{TR} (equation 4.2) derived. Errors were found to be as great as 0.02 deg/decade in the 15-year LTP and in 20-year LTP 0.015 deg/decade.

This results in error of $> 50\%$ for estimated T_{TR} over some time periods. Greatest errors are seen during time periods where the LS channel does not represent the MT channel layer above the tropopause (MT(ATROP)). This is when there is strong cooling in the stratosphere coincident with the ZTL above the tropopause. These results are for analyzed global averages. There may be other situations however when other latitudinal averaged temperature trends are analyzed that may show strong cooling/warming in the stratosphere and the ZTL above the chosen tropopause where misrepresentation of tropospheric temperature trends would also exist.

Finding coefficients for an LS/MT combination is training dataset dependent, as expected. JF06 found coefficients larger than those found with the database used in this work. As radiosonde data become more robust or stable, coefficients derived (FJWS, JF06, this work) seem to be decreasing, producing smaller estimated tropospheric temperature trends.

RATPAC(RW) is found that, during the MSU era, using 20-year or greater LTP, errors are small enough that conclusions from using an LS/MT combination is valid. This technique is however database dependent and would require that each database used be checked thoroughly to determine magnitude of errors before use with MSU data to estimate tropospheric temperature trends accurately. Any statistical combination still depends on the accuracy of RSS and UAH data therefore; discrepancies between these two data bases need to be resolved. This is considered in chapter 5.

CHAPTER 5

LIMITED TIME PERIOD COMPARISON UAH/RSS

5.1 Introduction

The United States Climate Change Science Program's (CCSP) *Temperature Trends in the Lower Atmosphere: Steps for Understanding and Reconciling Differences* [Karl, et al., 2006] is a comprehensive look into atmospheric amplification (greater warming in troposphere than at the surface) discrepancies between observations and models. They used RSS and UAH MSU databases which produce different temperature trend results for their respective channels (LS, MT, LT). Differences in these trends are caused by different data merging methods and differences between the diurnal adjustments that are used to account for orbital drift of the satellite [Mears, et al., 2006]. The purpose of this chapter is to implement the CCSP's recommendation and diagnose the relative merits of different merging methods for satellite data over LTP where the largest discrepancies between satellites and radiosonde data are found.

Recent studies documented differences between the UAH and RSS data sets [Christy and Norris, 2006; Christy, et al., 2007; Mears, et al., 2006; Mears and Wentz, 2005] and found that the likely primary cause of differences between the two groups in the LT and MT channels are the on-board calibration target parameters calculated by each group (due to different choices of overlap periods of the satellites used to create the time series). Methods to determine diurnal correction were found as a secondary issue. The CCSP addressed discrepancies in satellite trends and methods for creating temperature anomaly time series. Their recommendation was to diagnose the relative

merits of different merging methods for satellite data over limited time periods where the largest discrepancies between satellites and radiosonde data are found [Mears, *et al.*, 2006]. In this chapter the limited time periods (LTP) used are running 5- and 10-year least squares fit trends of various difference time series created from RSS and UAH MSU data.

A linear fit to the entire long term trends of RSS and UAH data may not be the best technique to diagnose differences in merging methods. Comparing the data over shorter, or LTP, affords the opportunity to determine how corrections for time dependent effects, such as orbital changes, affect the data for the actual time period over which they are applied. Any similar discrepancies among the merging methods found over more than one LTP may in addition resolve problems from a single process used over those time periods. These similar discrepancies may not even be seen using one long term linear trend.

Using difference time series removes any variability that may be common to both data sets and isolates those differences that are due to differing data set production methods or temperature measurement methods [Wigley, 2006]. Thus, any LTP trend anomaly indicates those time periods where differences in data set production methods are isolated.

5.2 Methods

Difference time series were created from the UAH and RSS MT and LT channels in two different ways. UAH data were subtracted from RSS data for each channel (RSS(LT)–UAH(LT) and RSS(MT)–UAH(MT)). Analyzing LTP on this type of

difference series leads to locating discrepancies found between the two groups in the same channel. Figure 5.1 shows an example of LTP on this type of difference series. Figure 5.1a and 5.1b show the difference time series RSS–UAH for MT and LT channels for global (a) and tropical (b) anomalies over land. The 10-year LTP for these difference series are shown in part (c) and (d) respectively. For global data (Figure 5.1c), the 10-year LTP trends in the MT channel are fairly constant, while in the LT channel they are quite variable. The reason for the variability is seen in the difference time series (Figure 5.1a) as a slow increase in the LT difference anomalies from 1989 to mid 1994 and general slow decrease from mid 1994 to 2003. This feature is in the LTP trend curve where the maximum 10-year trend is from 1989 to 1999 (shown as centered on 1994 in Figure 5.1c) and the relative minimum 10-year trend is from 1993 to 2003 (centered on 1998 in Figure 5.1c).

It is important to show that the LTP trends are capturing what can appear to be an obvious feature in the MSU difference time series. Some of the difference time series created do not have such an obvious signature, yet discrepancies are apparent when LTP trends are accomplished. This increases the confidence that the LTP method is robust in capturing the differences present between each group's data sets, a point which becomes more vital when radiosonde data comparisons are made (see section 5.3).

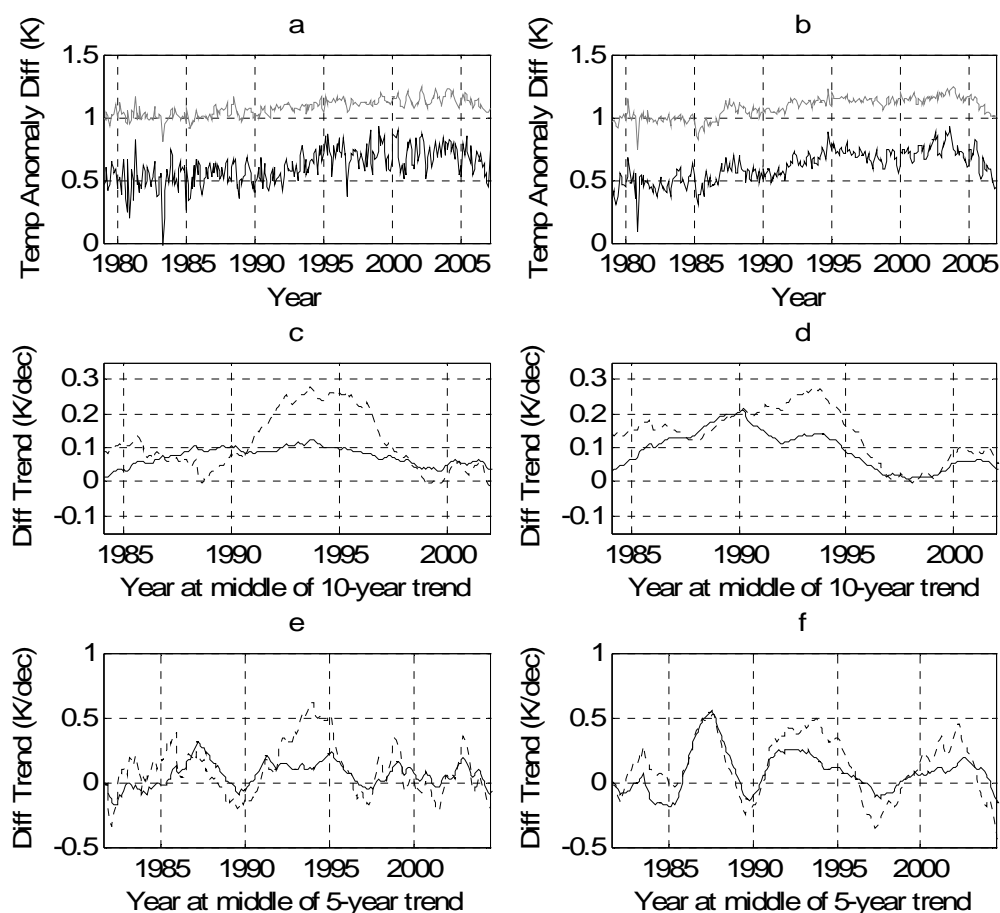


Figure 5.1 (a) RSS(MT)-UAH(MT) (grey offset by 1.0) and RSS(LT)-UAH(LT) (black offset by 0.5) temperature difference anomaly time series for global data over land, (b) tropical data over land. (c) 10-year Limited Time Period (LTP) trends of difference time series for global data; LT(dashed) MT(solid), (d) tropical data LT(dashed) MT(solid). (e) 5-year LTP trends of the difference time series for global data; LT (dashed) MT(solid), (f) tropical data; LT (dashed) MT(solid). Greatest discrepancies between groups are in the LT channel.

Difference trends were also created by subtracting the MT channel from the LT channel for each group ($RSS(LT) - RSS(MT)$ and $UAH(LT) - UAH(MT)$). LTP trends completed on this type of difference series results in locating differences in the trend tendency between the channels (LT and MT) within each group. It is possible to see variations in this type of difference series due to the different temporal variability of each channel's trend, however, as each group is using the same raw data any departure in the LTP trends, between the two groups, would indicate a time period where processing methods differ, not something physically happening in the atmosphere. Additionally, any discrepancies found in this type of difference series indicates time periods where different correction methods between the MT and LT channels were used, as opposed to a constant correction between the LT and the MT channel (within each group), discussed further in section 5.3.

In summary LTP trends on time series created from RSS–UAH for both MT and LT channels and LT–MT for both RSS and UAH were calculated. This was done for global and tropical data for land and ocean.

5.3 Results and Attribution

In order to assign attribution to results found in the LTP, methods used in creating each group's time series are briefly discussed and then results and attribution to those methods are discussed.

5.3.1 Review of correction/merging methods

Significant contributions to the uncertainty in satellite estimates of trends for MSU data sets result from corrections for orbital drifts resulting in different diurnal

sampling times, and different methods of merging data from the different satellites [Mears, *et al.*, 2006].

To correct for diurnal drift in the each of the satellites, both groups first average together the ascending and descending orbits [Mears, *et al.*, 2006]. This removes the first harmonic of the diurnal cycle. Each group then uses a different method for removing the higher order harmonics of the diurnal cycle.

The UAH group calculates mean differences, arising from different measuring times, by subtracting the temperature measurements on one side of the satellite track from the other [Christy, *et al.*, 2000; Mears, *et al.*, 2006]. As these two measurements are for different local times, this allows for a calculation of the change in measurements as a function of time. Additionally, different adjustments are used for land and ocean. This leads to an averaged diurnal adjustment to be made for each zonal band.

The RSS group, on the other hand, uses hourly output from a climate model which enables adjustments at the same resolution as the data [Mears, *et al.*, 2006]. It is important to note that the diurnal corrections for each channel are created separately¹, thus any discrepancy in the MT channel correction is separate from any discrepancy in the LT channel correction. The diurnal corrections are applied to the raw data before any merging or target corrections are completed.

After the diurnal corrections are applied, the data from different satellites in orbit at any given time are merged together to create one time series for each channel.

¹ Since the two channels, LT and MT, have different vertical weighting functions, any effects that vary in the vertical, such as diurnal temperature changes, would affect each channel differently

To accomplish this each group must remove calibration drifts that are determined from the on board hot calibration target and correct for offsets found by comparing co-orbiting satellites [Christy, et al., 2000; Mears, et al., 2006; Mears, et al., 2003]. Each group removes the calibration target temperature effect using a model that includes a constant offset for each satellite, and an additional empirical “target factor” multiplied by the calibration target temperature. The diurnal correction for each channel has already been added to the raw data before the regression procedure is accomplished to create the target factor and offset. Any errors present in the diurnal correction therefore will influence the merging coefficients [Mears and Wentz, 2005]. RSS uses all available data from overlapping satellites in the regression procedure while UAH uses only satellite overlaps with durations longer than 2 years. UAH removed three periods of data that showed insignificant variance when overlapping with co-orbiting satellites [Christy, et al., 2000]. These were TIROS-N in its overlap with NOAA-6 (July-December 1979), NOAA-10 in its overlap with NOAA-11 (October 1988-August 1991), and NOAA-12 with its overlap with NOAA-11 (September 1991-March 1995).

5.3.2 Results and Attribution

Analyzing several combinations of difference time series helped us narrow our focus for further analysis on those combinations that have the greatest discrepancies. Figure 5.1 shows 10-year LTP trends from the RSS(MT)–UAH(MT) and RSS(LT)–UAH(LT) temperature anomaly difference series for global (5.1c) and tropical (5.1d) data over land. As mentioned before, the trends for the MT channel are relatively constant while there is considerable variability in the LT channel trends for the global

dataset. The tropical data show trends in the LT channel to be consistent with the MT channel until trends centered on 1990, when they depart and the LT trends become variable as seen in the global case. As previously indicated, departures in the LTP trends between the two groups are due to differences in construction methods and not physical changes in the atmosphere; therefore, we are able to state that the differences in correction method by one or both of the group's LT channel is indicated by the variability in trends. Figure 5.2 compares 10-year LTP global trends for the RSS(LT)–UAH(LT) temperature anomaly difference series over ocean and land. Here there are relatively small changes in trends over the ocean as opposed to the high variability in trends over land. This indicates the greatest discrepancies between RSS and UAH are not only in the LT channel, but over land as well.

One of the greatest discrepancies is a departure seen in the 5-year LTP trends centered on July 1987 in the tropics (Figure 5.1f). This departure is caused by the difference in the target parameters used for the NOAA-9, which was only in service for 2 years and poorly determined due to its short overlap with other satellites [*Mears and Wentz, 2005*]. The departures in trends are seen to be similar in both the MT and LT channels in the tropics and relatively small in the global trends. Because of this, we were unable to determine any other information and will continue to analyze discrepancies found in trends that are not affected by these NOAA-9 corrections. This includes 10-year trends centered on 1993 and after and 5-year trends centered on mid-1989 and after.

The greatest discrepancy in the 10-year LTP trends are those in the LT channel centered on 1993 through those centered on 1995 in both global and tropical data (Figures

5.1c, 5.1d)). The largest discrepancies for 5-year LTP trends are those in the LT channel centered on 1993 in both global and tropical data, and also in the tropics we see a significant departure in LT trends again centered on 1997, 2002 and 2004.5 (Figure 5.1f). The best example in a difference series is the tropical difference series shown in Figure 5.1b. Here we see $RSS(MT)-UAH(MT)$ compared to $RSS(LT)-UAH(LT)$ over land, and the signatures that cause the rapid LT trend departures in Figure 5.1(d) are seen by the larger increase in difference anomalies from 1989 to 1995 as compared to the MT channel. This is over the time period where the corrections for NOAA-11 are accomplished. Signatures causing trend variability are also seen by the moderate decrease in difference anomalies from 1995 to 1999 when corrections for NOAA-12 are accomplished. After 2000 there is another larger increase in LT difference anomalies during the period when NOAA-14 merging parameters are introduced into the time series and a sharp decline in anomalies from 2004 thru 2006 when NOAA-15 parameters are applied. The increases and decreases in the LT difference time series correspond to the maxima and minima in the LTP trends which correspond to what appears to be signatures in the shape of the diurnal corrections of the NOAA-11 thru NOAA-15. Figure 5.3 compares the $RSS(LT)-UAH(LT)$ (global, land) difference time series (5.3a), the $RSS(LT)-UAH(LT)$ (tropical, land) difference time series (5.3b) with the RSS globally averaged diurnal correction for NOAA-11 (5.3c), NOAA-12 (5.3c) and NOAA-14 (5.3d) over their respective time periods. Here we're showing the correction signatures are of diurnal shape and are still evident in the difference time series. However, the shape of

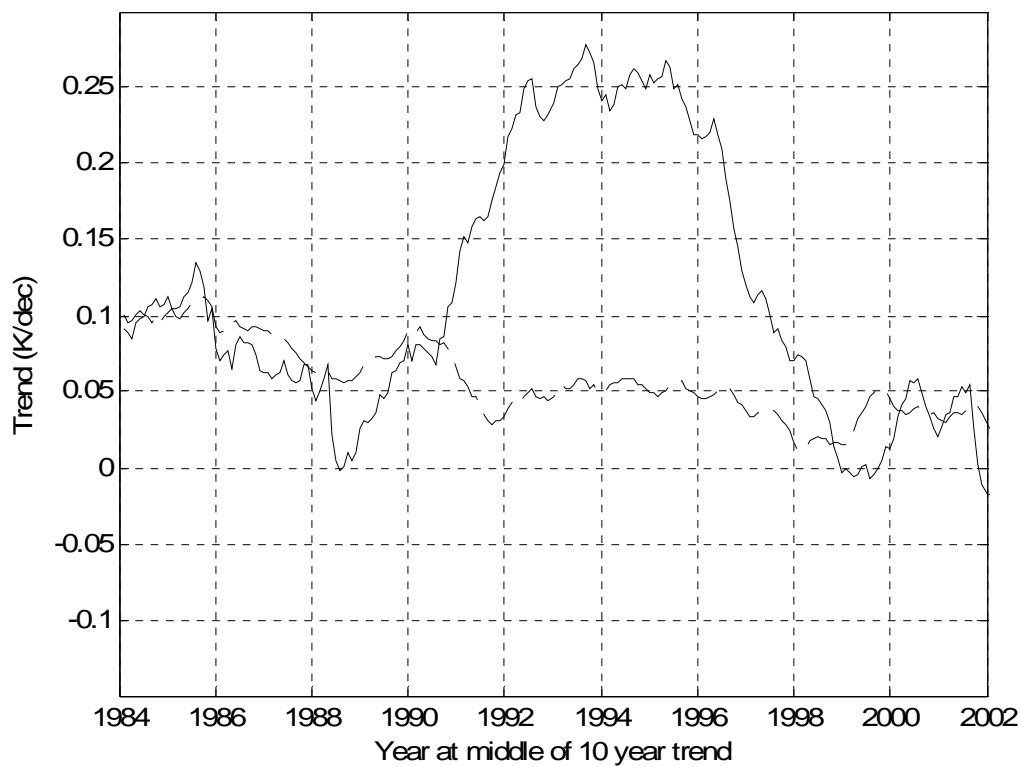


Figure 5.2. 10-year LTP global trends for the RSS(LT)–UAH(LT) difference series over ocean (dashed) and land (solid). Largest discrepancies in the LT channel are over land, indicating that diurnal correction may be cause.

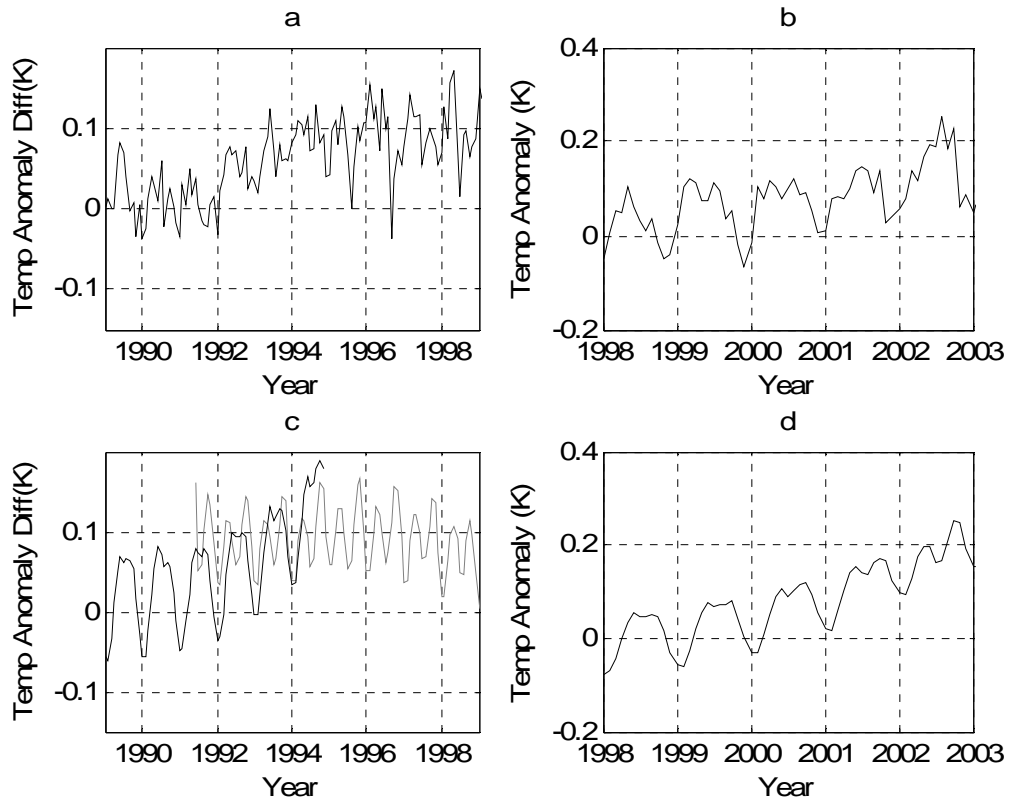


Figure 5.3. RSS(LT)-UAH(LT) (a) Global difference time series (RSS(LT)-UAH(LT)) over land 1989-1999 (b) Tropical difference time series over land 1998-2003. (c) RSS global average diurnal correction for NOAA-11(black) and NOAA-12(grey) 1989-1999. (d) RSS global average diurnal correction for NOAA-14 1998-2003. The shape of the diurnal corrections are evident in the difference time series.

the diurnal correction and the target temperature drift are the same [*Christy, et al., 2000; Mears, et al., 2003*] indicating the discrepancies can arise from either the actual diurnal correction or the derived target factors.

The target factors are constants that describe the behavior of the radiometer and are determined using the MT channel data with the diurnal correction already applied [*Christy, et al., 2000; Mears and Wentz, 2005*]. These coefficients can be applied to other linear combinations of the MT channel including the LT channel. Both groups accomplish this in the creation of their final series with slight variations between MT and LT target factors in UAH data. Because the target parameters are nearly constant between channels (indicating they're the same over land and ocean), if they were the primary cause of the discrepancies found we would expect to see the same variation in LTP trends created from channel differences over ocean as we have seen over land. As seen in Figure 5.4, this is not the case. Here the difference series $RSS(MT) - UAH(MT)$ and $RSS(LT) - UAH(LT)$ are compared for 10-year LTP over land (5.4a) and over ocean (5.4b) (for 5-year LTP (5.4c) and (5.4d) respectively). Discrepancies are significantly different for the LTP trends over land than ocean, which is not consistent with discrepancies being caused by target factors, but more in line with diurnal corrections. Diurnal corrections should be larger over land and in the LT channel than over ocean and in the MT channel since diurnal temperature variations are greater over land, and decrease with height. An additional test to eliminate target factors as the primary cause of discrepancies is to compare difference series created by subtracting channels in each group; ($RSS(LT) - RSS(MT)$ and $UAH(LT) - UAH(MT)$). Discrepancies created by the

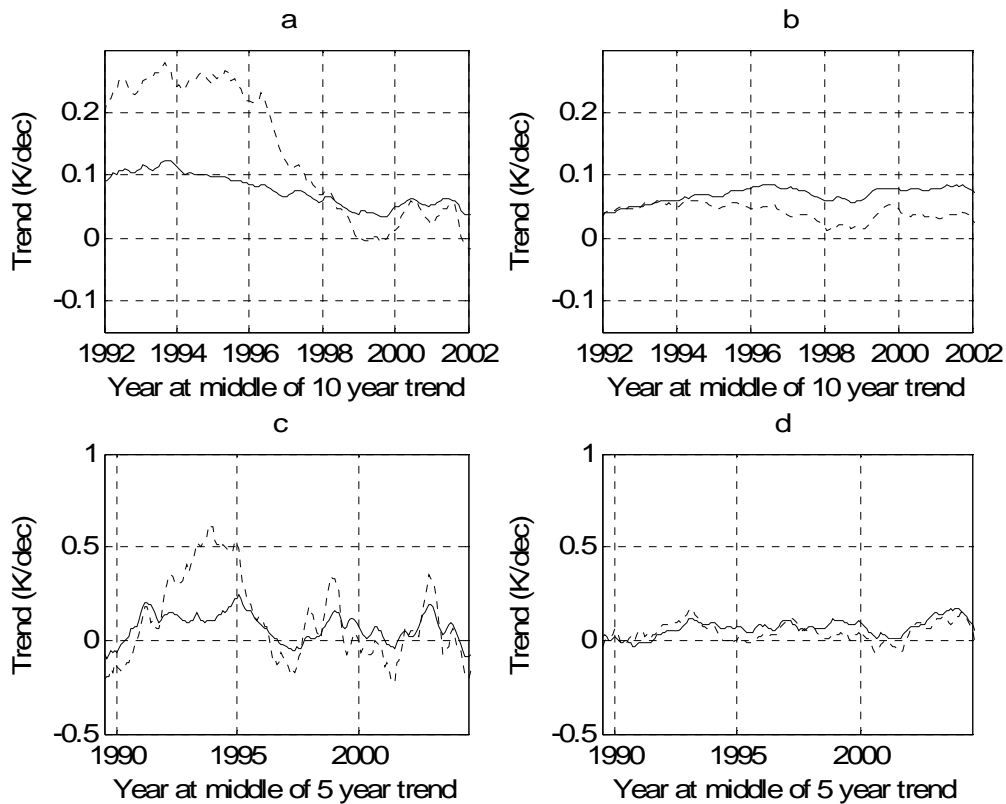


Figure 5.4. (a) Limited Time Period (LTP) trends on RSS(MT)–UAH(MT) (solid) and RSS(LT)–UAH(LT) (dashed) for 10-year LTP global land, (b) ocean. (c) 5-year LTP global land and (d) ocean. Greatest differences between databases are in the LT channel over land.

target factors and offsets are minimized in this type of difference series as they are nearly constant in both channels, therefore, any discrepancies seen, between groups, are caused predominantly by diurnal corrections. Figure 5.5 shows the difference series $RSS(LT) - RSS(MT)$ and compares to $UAH(LT) - UAH(MT)$ for 10-year LTP over land for global (5.5a) and tropical (5.5b) data. Departures between the two group's databases are seen and, because this difference series shows primarily diurnal correction discrepancies, we are able to conclude that the departures are dominated primarily by the diurnal correction discrepancies. This is expected as the greatest discrepancies are found over land in the LT channel both of which have the greatest diurnal cycle and thus greatest corrections required. It is important to note here that this does not indicate which group's diurnal correction procedure may be causing the departure in trends.

As shown above differences in the LT channel are most likely the primary cause of the departures, however the signatures in this type of difference series can be caused by the UAH method underestimating the diurnal correction or the RSS method overestimating the diurnal correction or a combination of both. This will be discussed further when the MSU and Radiosonde data are compared in section 5.3.

At first our findings may appear to be in complete opposition to the CCSP key findings that for the tropospheric satellite data (MT and LT), the primary cause of trend discrepancies is from differences in merging methods [Mears, *et al.*, 2006]. However, with an expanded definition our findings may be considered consistent with the CCSP findings in the MT channel. Differences in derived target parameters have been

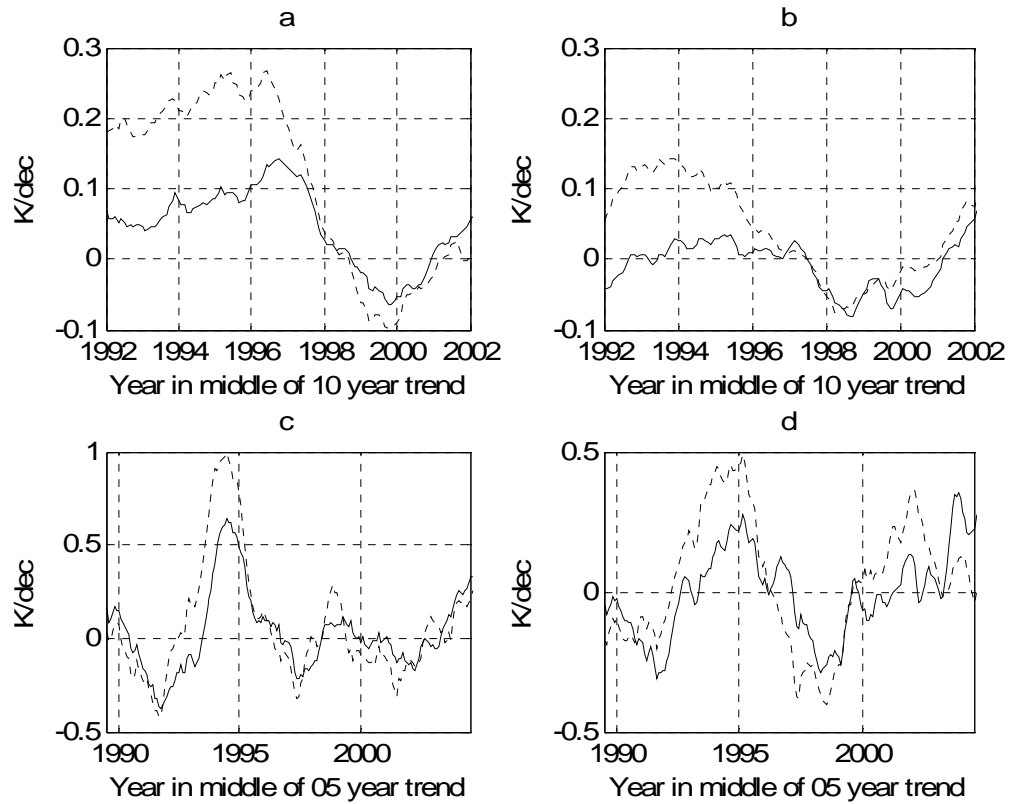


Figure 5.5 (a) 10-year LTP trends on UAH(LT)-UAH(MT) (solid) and RSS(LT)-RSS(MT) (dashed) for global, (b) tropics. (c) and (d) same as (a) and (b) for 5-year LTP trends. The greatest discrepancies from this type of difference series shows where different diurnal correction methods affect the data.

explained as resulting from the two group's data choices for the regression procedure [Mears and Wentz, 2005]. UAH uses only satellite overlaps with durations longer than 2-years while RSS uses all available data from overlapping satellites. Our findings however may be consistent with the CCSP in the MT channel if the total discrepancies created by the final target factors are further defined by two separate causes: (1) discrepancies resulting strictly from the method in which overlaps were selected and (2) discrepancies resulting from differences in the diurnal correction. Mears and Wentz [2005] found that MT channel data over ocean are best for determining target parameters due, in part, to a greater diurnal cycle over land than for over ocean. As the total diurnal-shaped correction includes both the diurnal correction and the target parameters any overestimated/underestimated diurnal correction, including initial discrepancies, would have to be compensated by a smaller/greater target parameter (bias plus target temperature factor). Thus, the mere fact that the final target factors are different can be explained by an initial discrepancy in diurnal corrections and not necessarily the selection of the overlap of satellites alone. In reality it is likely a combination of both, but the correction dominating the discrepancy appears to be different for each channel (MT/LT).

The present findings show that the diurnal correction dominates the discrepancies in the LT channel, however, it is in addition to differences in target bias parameters since Christy et al., [2007] determined that steps between the databases exist during some of the LT time periods. Determining which parameter dominates MT channel discrepancies is more difficult, mainly due to the target parameter's dependence on the initial diurnal correction. The total discrepancies in the difference time series are combinations of

differences in diurnal corrections and differences in target parameters and the fact that the diurnal correction is smaller in this channel. The differences in target parameters result from differences in choice of overlap and differences in diurnal correction. This indicates that an initial discrepancy from the diurnal correction will not only be present in the final data series but be in addition to the discrepancy created by its contribution to the target parameter correction. As the diurnal correction method is over or underestimating the diurnal correction in the LT channel, it follows that the same process is invoking a discrepancy in diurnal correction in the MT channel. The difficulty lies in the fact that the target parameter determination is dependent on the diurnal correction applied. However any signatures found in LTP trends in the MT channel are not large enough to extract any concrete information. An initial over or underestimation of the diurnal correction in the MT channel may be small enough to either be masked or dominated by the target factors.

As stated previously the LT diurnal correction discrepancies can either be explained by an overcorrection to the database by the RSS group or an undercorrection by the UAH group (seen by order of subtraction in difference series) or a combination of both.

5.4 Radiosonde Comparison

To compare the UAH and RSS data sets, we use the anomaly difference series created by subtracting channels of each group ($RSS(LT) - RSS(MT)$ and $(UAH(LT) - UAH(MT))$). This type of difference series was used for two reasons. First, using the two channels created by the same instrument (MSU or Radiosonde) helps to

eliminate any structural inconsistencies. Second, this difference series compares predominantly diurnal inconsistencies between the groups as discussed previously. We also create the same type of difference series from simulated channels using a static weighting function [*Christy, et al., 2003*] on an independently derived radiosonde dataset. Used here are RATPAC-B radiosonde data based on the temporally homogenized data set described in Free et al., [2005]. Randel and Wu [2006] found jumps and discontinuities in individual station records that are used in the RATPAC-B data causing a tendency for spurious cooling in stratospheric and tropospheric data. For this reason, we used only those radiosonde sites and times that were found to be “good” by this study, minimizing a long term cooling bias in the results of the comparison (RATPAC(RW)).

The three difference series (MT–LT for UAH, RSS and Sonde data) are shown in Figure 5.6a for 10-year LTP trends (global land) and (5.6b) for 5-year LTP trends (global land). The LTP trend series created from the radiosonde data follows the UAH better for both 10-year and 5-year LTP trends. The strong departure in trends of the RSS data vs UAH and Sonde data are consistent with the time periods the diurnal correction dominates the LT channel. Although we used “good” radiosonde data [*Randel and Wu, 2006*] in order to minimize negative biases in the radiosonde data, biases may still exist in the data during some time periods. Sonde data follows the UAH data most closely for 5-year and 10-year trends; therefore, coincidence of agreement between datasets where a long term negative bias through time still exists is unlikely, especially in the 5-year LTP trends. In addition, there may be a slight bias induced in the comparison as both groups use slightly different methods to categorize land anomalies.

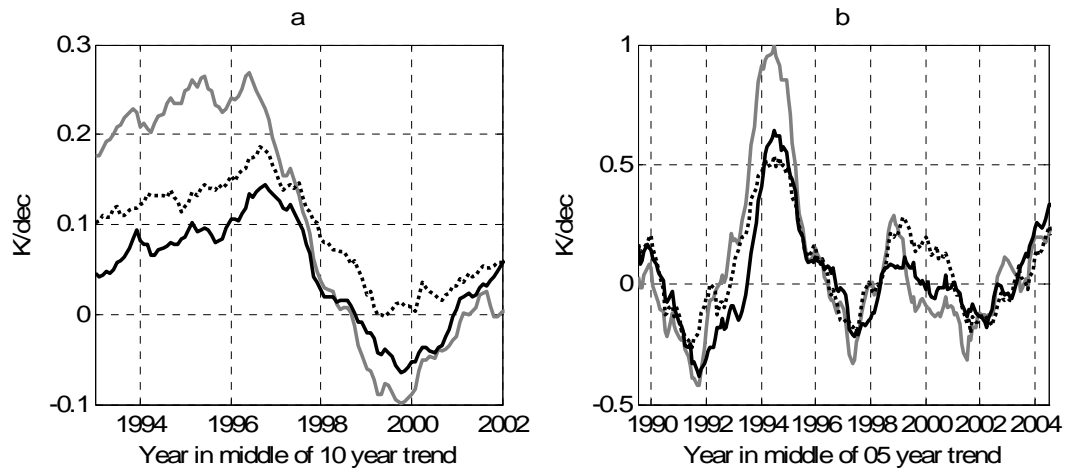


Figure 5.6 (a) 10-year LTP trends on UAH(LT)-UAH(MT) (solid), RSS(LT)-RSS(MT) (grey) and Sonde(LT)-Sonde(MT) (dashed). (b) Same as (a) with 5-year LTP trends.

Sonde data follows UAH more closely thus the possibility of long term biases still in the sonde data is unlikely.

Difference series were made from the difference series shown in Figure 5.6 ((Sonde(LT)-Sonde(MT)) – (UAH(LT)-UAH(MT)) and (RSS(LT)-RSS(MT)) – (Sonde(LT)-Sonde(MT))) accounting for autocorrelation correction using methods in Santer et al. [2005] and are shown in Figures 5.7 and 5.8. Here the differenced series with the 95% CI is seen. In Figure 5.7 it is seen that the 10-year trends center on the mid-1994's through 10-year trends centered on the mid-1995's the RSS–Sonde trends are significantly different than zero where the Sonde–UAH trends are not. In addition, for 10-year trends centered in late-1999 through 10-years trend centered in early-2000 RSS–Sonde trends are significantly different from zero where Sonde–UAH are marginally not. Another key feature in the RSS–Sonde series is the rapid departure in trend magnitude from trends centered in 1995 to trends centered in late-1999 where in the Sonde–UAH data the magnitude in trends is relatively constant. These features are consistent with the diurnal correction signatures previously discussed. Figure 5.8 shows the 5-year trends for the tropics over land. RSS–Sonde trends are significantly different from zero for trend centered on beginning-1998 through trends centered on beginning-1999 where Sonde–UAH trends are marginally not. In addition RSS–Sonde was significantly different from zero for trends centered on late-2001 to trends centered on mid-2002 where Sonde–UAH trends are not. These findings indicate the RSS method for creating the diurnal correction (use of a climate model) is the primary cause for the discrepancies between RSS and UAH databases in the LT channel.

Causes of errors are likely due to the inability of the climate model, used by RSS to evaluate diurnal effects, to represent accurately the diurnal cycle or include diurnal

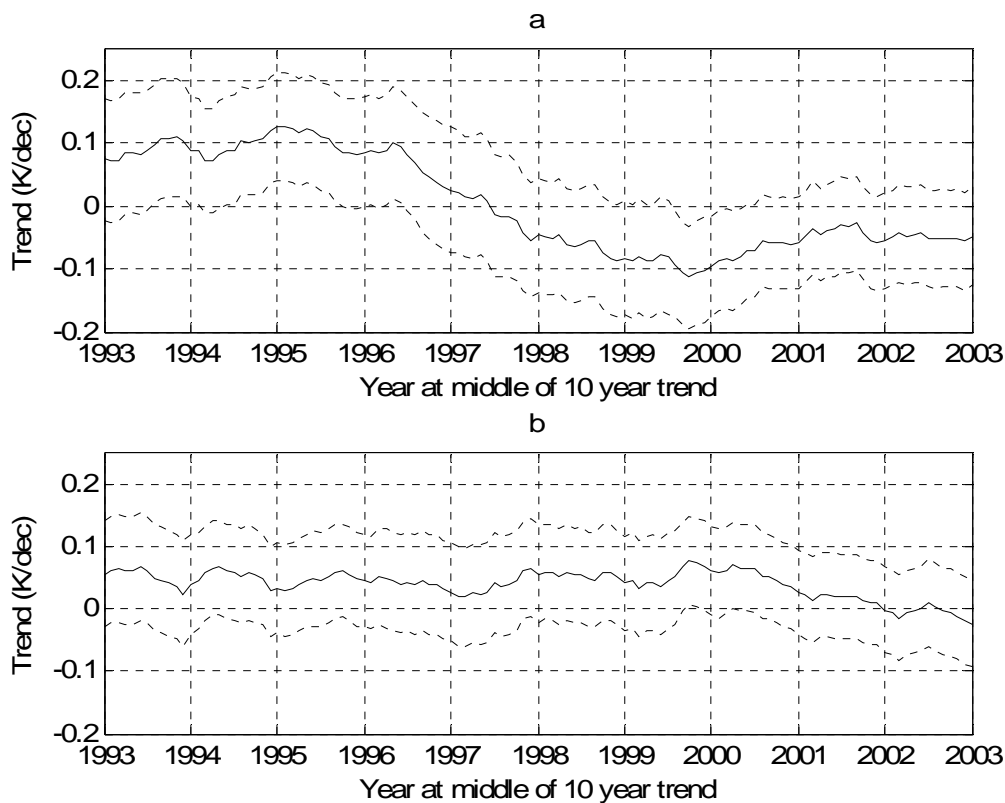


Figure 5.7 (a) Differences from difference series created in Figure 5.6. 10-year LTP trends for $(RSS(LT)-RSS(MT)) - (Sonde(LT)-Sonde(MT))$ (global, land) and (b) $(Sonde(LT)-Sonde(MT)) - (UAH(LT)-UAH(MT))$. Dashed lines around each are the 95% CI. The Sonde–UAH series is not significantly different from zero while there are time periods where the RSS–Sonde is significantly different from zero. These time periods are consistent with time periods where the greatest discrepancies caused by diurnal corrections are present.

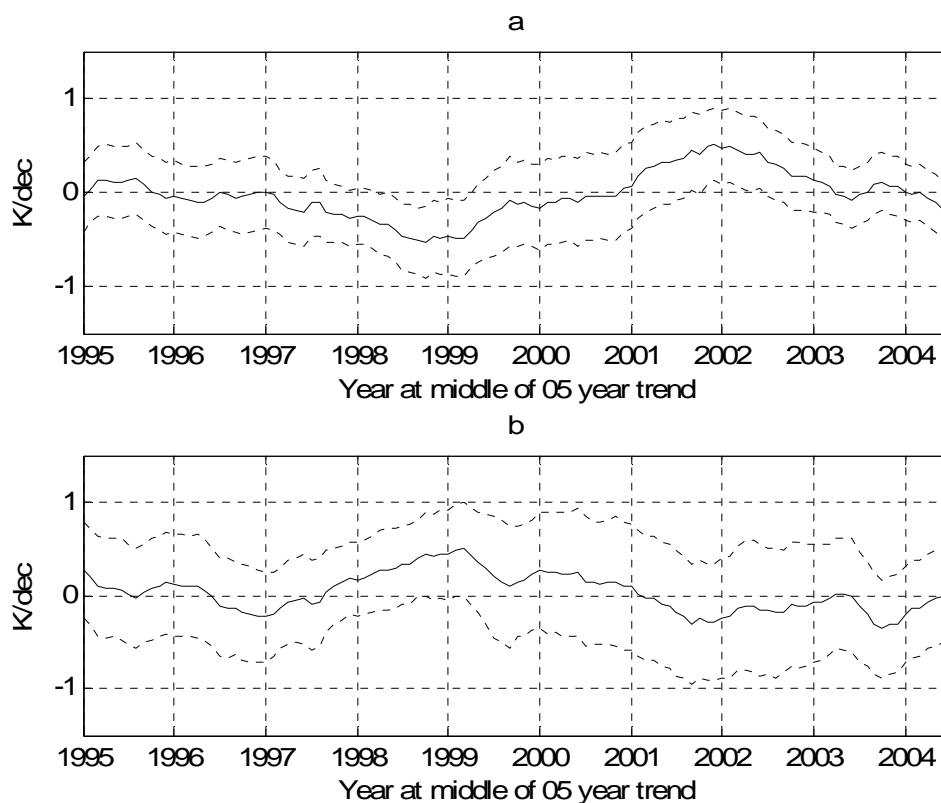


Figure 5.8 (a) Differences from difference series created in Figure 5.6. 5-year LTP trends for $(RSS(LT)-RSS(MT)) - (Sonde(LT)-Sonde(MT))$ (tropics, land) and (b) $(Sonde(LT)-Sonde(MT)) - (UAH(LT)-UAH(MT))$. Dashed lines around each are the 95% CI. The Sonde–UAH series is not significantly different from zero while there are time periods where the RSS–Sonde is significantly different from zero. These time periods are consistent with time periods where the greatest discrepancies caused by diurnal corrections are present.

variability for surface temperature [*Dai and Trenberth, 2004; Mears, et al., 2006*]. However, if the diurnal temperature range has decreased over time [*Braganza, et al., 2004; LaDochy, et al., 2007*] then a mean diurnal amplitude created from a 5-year time period (1979-1984) will be greater than any diurnal amplitude created after that time period. Using a correction based on this earlier time period would overestimate the diurnal correction needed in a later time period. This is what is done by the RSS method and may also be a plausible explanation.

We cannot count out that the UAH results may still have errors in the method since their diurnal correction is sensitive to satellite attitude errors and uses latitudinal averages [*Mears, et al., 2006; Mears and Wentz, 2005*]. At this time we are unable to see any significant signatures that would indicate comparable differences when each database is compared to radiosonde data.

5.5 Summary and Conclusions

The use of LTP trends on various difference time series created from UAH and RSS MT and LT channels has been shown to indicate the greatest discrepancies between these two databases are over the time periods when correction methods for NOAA-11 thru NOAA-15 are accomplished. The greatest discrepancies have also been shown to be in the LT channel and most prominent over land, primarily caused by corrections made to eliminate diurnal drift signatures.

At first these findings may appear to be in complete opposition to the key CCSP findings that for the tropospheric satellite data (MT and LT), the primary cause of trend discrepancies is from differences in merging methods [*Mears, et al., 2006*]. These

findings may be consistent however with the CCSP findings in the MT channel if the total discrepancies created by the final target factors are further defined by two separate causes: (1) discrepancies resulting strictly from the method in which overlaps were selected and (2) discrepancies resulting from differences in the diurnal correction. As the total diurnal-shaped correction includes both the diurnal correction and the target parameters any overestimated/underestimated diurnal correction, including initial discrepancies, would have to be compensated by a smaller/greater target parameter (bias plus target temperature factor). Thus, the mere fact that the final target factors are different can be explained by an initial discrepancy in diurnal corrections and not necessarily the selection of the overlap of satellites alone. In reality it is likely a combination of both, but the correction dominating the discrepancy appears to be different for each channel.

It has been shown that the diurnal correction dominates the discrepancies in the LT channel, however they are in addition to differences in target bias parameters [Christy, *et al.*, 2007]. Which parameter dominates MT channel discrepancies is more difficult to determine, mainly due to the target parameter's dependence on the initial diurnal correction. This dependence indicates that an initial discrepancy from the diurnal correction will not only be present in the final data series but be in addition to the discrepancy created by its contribution to the target parameter correction. As RSS's method is overestimating the diurnal correction in the LT channel, it follows that the same process is invoking a discrepancy in the diurnal correction in the MT channel. An initial overestimation of the diurnal correction may be small enough to either be masked

or dominated by the target factors in the MT channel, but further research is necessary to isolate which correction method is dominant, if any.

The MSU data were compared to the radiosonde data and found that the RSS-Sonde is significantly different from zero while Sonde-UAH is not during time periods that are consistent with the overcorrected diurnal corrections dominating the LT channel. Only “good” radiosonde data [Randel and Wu, 2006] are used in order to minimize negative trend biases in radiosonde data, however biases may still exist in the data. Sonde data follows the UAH data closely through most 5-year and 10-year trends, and this coincidence of agreement is unlikely between datasets where a long term negative bias through time still exists, especially in the 5-year LTP trends. The corrected diurnal signatures still exist in the RSS LT time series and in the longer 10-year LTP trends we see a positive bias, thus the present corrected diurnal signatures are likely affecting the long term trend with a warm bias.

Causes of these diurnal errors are likely due to the inability of the climate model, used by RSS, to accurately represent the diurnal cycle or include diurnal variability for surface temperature [Dai and Trenberth, 2004; Mears, et al., 2006]. However, if the diurnal temperature range has decreased over time [Braganza, et al., 2004; LaDochy, et al., 2007] then a mean diurnal amplitude created from a 5-year time period (1979-1984) will be greater than any diurnal amplitude created after that time period. Using a correction from an earlier time period would over estimate the diurnal correction needed during a later time period. This is what is done by the RSS method and may also be a plausible explanation. In any case these findings enhance the importance of

understanding temporal changes in the atmospheric temperature trend profile. This understanding would further lead to insight into temporal changes in vertically integrated diurnal cycles. The implications on multiple climate studies using these data series include the current quest to understand model vs. observation differences in atmospheric amplification.

CHAPTER 6

ATMOSPHERIC AMPLIFICATION

6.1 Globally Averaged Atmospheric Amplification

In order to assess how the aforementioned findings integrate into interpreting atmospheric amplification (greater warming in the troposphere than at the surface) Figure 6.1 shows estimated tropospheric temperature trends using coefficients found with NoCONST25 and JF06OLD (see Table 4.1) methods using RSS and UAH datasets. In addition, estimated tropospheric temperature trends using RH07 method on the UAH dataset are included. UAH and RSS LT channels are included as a means to estimate if amplification of temperatures is evident in MSU data. Twenty five-year surface temperature trends (GHCN-ERSST and HadCRUTv2) are included for comparison purposes.

If amplification is happening in the atmosphere as prescribed by most models then the entire troposphere would have the greatest trend followed by the LT channel and then the surface would have the least trend out of the three channels.

Using the RSS data it is seen that the greatest trends are those in the LT channel followed by the entire troposphere then surface. For UAH the greatest trends are those at the surface with the LT channel similar or less than the surface trends. The estimated UAH tropospheric temperature trends show the least warming in this database (Figure 6.1). RSS data suggest that amplification is happening but not up to 200 hPa as prescribed by physics and the models. RSS data indicate amplification up to around ~300-500hPa (approximate depth of the LT channel) and a profile of less warming or

cooling above this level; seen from estimated tropospheric trends. For UAH data, indications are more constant temperature trends or less warming up to ~300-500hPa, then a profile of less warming or cooling above this level. Both databases show their respective estimated tropospheric temperature trends are less than the corresponding LT trend indicating that above the surface-300 hPa layer the atmosphere starts to show less warming or cooling. In fact, this is what is seen when one looks at the radiosonde 25-year LTP analysis (Figure 6.2). Here it is seen that the greatest warming over most time periods is in a ~300-500 hPa layer and less warming or cooling above this level exists.

Previously it was shown that in the 15-year LTP the ZTL was as far down as ~300mb. Even in the 25-year LTP trends (Figure 6.2) it can be seen that the ZTL is below 200 hPa (trends centered on ~1990). Variability in the lower level of the cooling layer in this manner shows that the layer between approximately 300hPa to 150hPa can contribute to either warming or cooling to the MT channel. As the LS channel only senses down to approximately 150hPa, it would not be able to represent the variability in this layer and shows why any statistical method using a LS/MT combination to estimate T_{TR} should not be used (see chapter 4), and the LT channel actually turns out to be the best channel to use, for studies of atmospheric amplification, using satellite data. In fact, the paradigm of using the tropopause for a boundary in studies of temperature trends in the atmosphere should shift to the layer where the transition between warming and cooling exist (ZTL) as they may not be coincident.

These findings indicate that we should look into the original theory and how models handle this theory. Either the peak in warming is ~300-500 hPa and the theory

needs to be revisited, or the theory is correct and climate forcing above this layer is continuing to modify where the peak should be (~200mb). In either case a comprehensive look into what modifies the temporal changes in the temperature trend profile should be at the forefront of future investigations. How the models are parameterizing these temporal changes need to be revisited, including those factors which determine the height of the ZTL.

Currently UAH data are likely more accurate than RSS (see chapter 5). This allows the conclusion, that using MSU broad atmospheric weighted channels, in addition to RATPAC(RW), atmospheric amplification is not happening in the atmosphere on a globally averaged data set during the MSU era. There is evidence however from the radiosonde data, as discussed, that show greater warming in the ~300-500 hPa layer than at the surface during some LTP in the entire radiosonde database. If indeed, the tropospheric amplification is not in agreement with model predictions, as indicated by this work, this also requires further study.

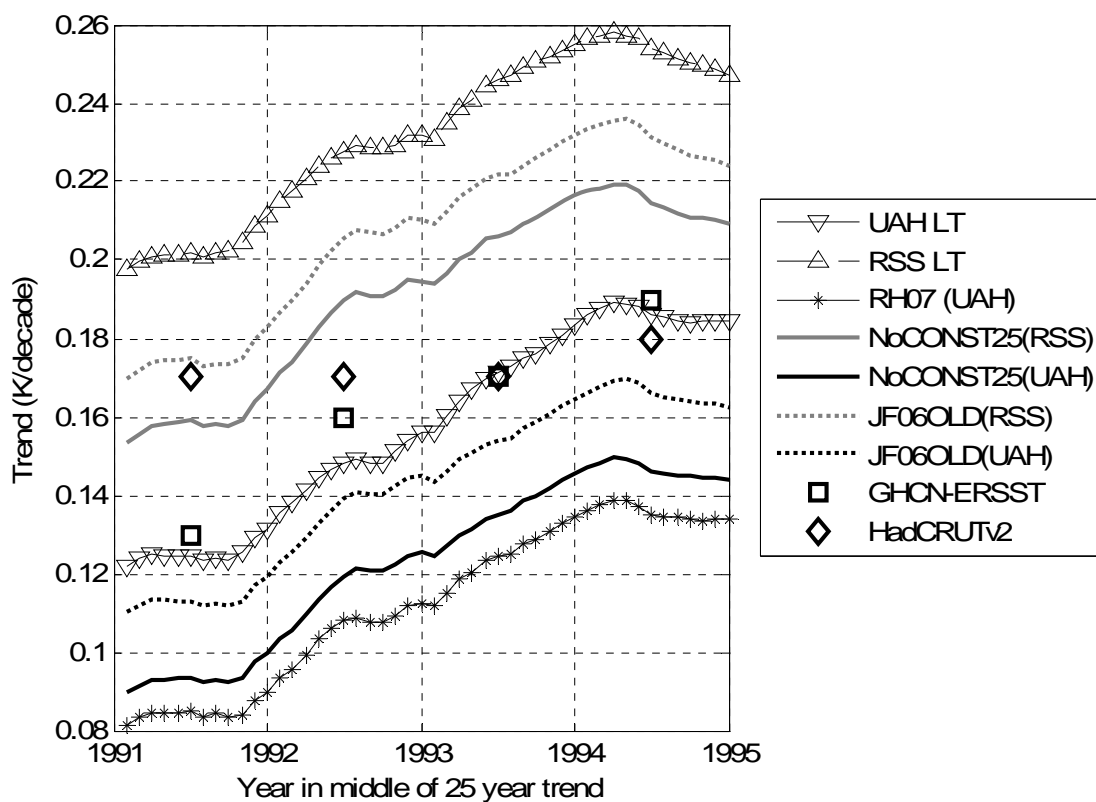


Figure 6.1 25-year LTP for estimated troposphere temperature trends (T_{TR}) using NoCONST25(solid), JF06OLD(dashed) with RSS(grey) and UAH(black) data. T_{TR} is also calculated using RH07 method with UAH data (black ---). UAH LT channel (inverted triangle) and RSS LT channel (triangle) are shown for atmospheric amplification comparison. GHCN-ERSST (square) and HadCRUTv2 (diamond) surface 25-year trends are also shown. Both databases show their respective estimated tropospheric temperature trends are less than the corresponding LT trend indicating that above the surface-300 hPa layer the atmosphere starts to show less warming or cooling. UAH data (likely more accurate than RSS) does not support atmospheric amplification during the globally averaged MSU era.

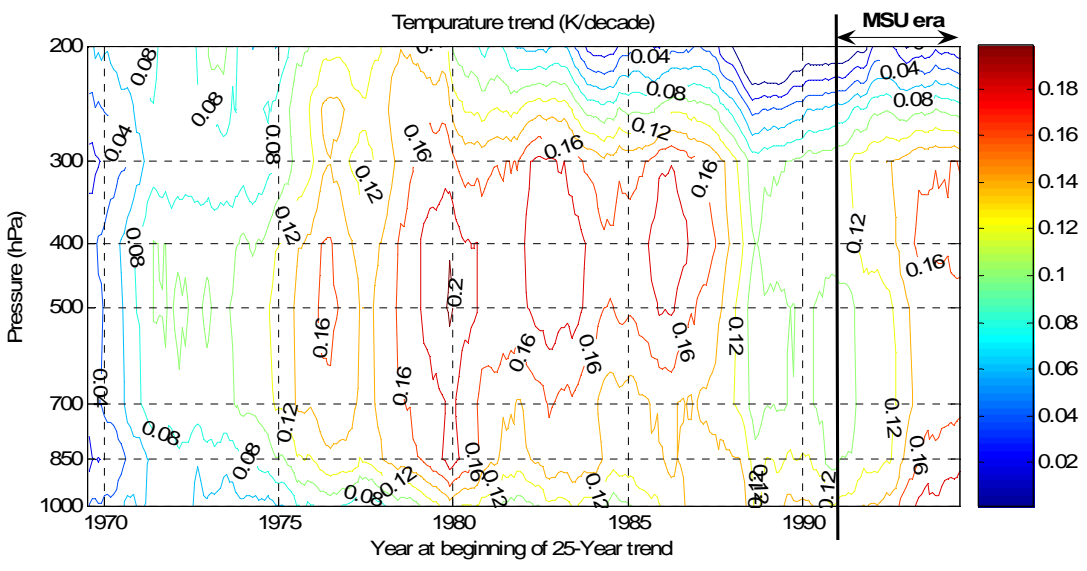


Figure 6.2 25-year LTP trends (K/decade) centered on 1975-1994.5 for a atmospheric layer 1000-200 hPa. Greatest warming is ~ 300-500 hPa; over the MSU era, trends centered on 1991.5-1994.5 one would not see atmospheric amplification.

CHAPTER 7

SUMMARY AND CONCLUSIONS

7.1 Summary and Conclusions

The objective of this study was to evaluate MSU derived temperature trend methods due to “the considerable disagreements between tropospheric datasets” (CCSP) so investigation into atmospheric variability is able to move forward.

The accuracy of using a statistical combination of the MT and LS channels to mitigate contamination from the stratosphere in the MT channel was probed using LTP analysis. LTP analysis were used on RATPAC(RW) data showing the ZTL is most variable through the layer where the combination of the weighing functions for the MT and LS channels have the greatest influence on the estimated tropospheric temperature. Greatest errors were between T_{TR} using *any* LS/MT combination method and the actual T_{TR} (equation 4.2) derived. Errors were found to be $> 50\%$ for estimated T_{TR} over some LTP. Greatest errors were coincident with time periods when there was strong cooling in the stratosphere and the ZTL was above the tropopause, indicating the LS channel does not represent the MT channel layer above the tropopause (MT(ATROP)).

I also found coefficients for an LS/MT combination is training dataset dependent, as expected. As radiosonde data become more robust or stable coefficients derived (FJWS, JF06, this work) seem to be converging to smaller coefficients, thus smaller estimated tropospheric temperatures. These results are for analyzed global averages. There may be other situations however when other latitudinal averaged (or any subset of global data) temperature trends are analyzed that may show strong cooling/warming in

the stratosphere and the ZTL above the chosen tropopause exist. Misrepresentation of tropospheric temperature trends is possible in any of these scenarios indicating that any statistical method using LS and MT channels is not recommended for LTP 25-years or less.

The use of LTP trends on various difference time series created from UAH and RSS MT and LT channels indicates the greatest discrepancies between these two databases are over the time periods when correction methods for NOAA-11 thru NOAA-15 are accomplished. The greatest discrepancies are shown to be in the LT channel and most prominent over land, indicating discrepancies arise from the diurnal correction.

The MSU data were compared to the radiosonde data and found that RSS–Sonde is significantly different from zero while Sonde–UAH is not during time periods consistent with the overcorrected diurnal corrections dominating the LT channel. Only “good” radiosonde data [*Randel and Wu, 2006*] are used to minimize negative trend biases in radiosonde data; however biases may still exist in the data. Sonde data follow the UAH data closely through most 5-year and 10-year trends, and this agreement is unlikely between datasets where a long term negative bias through time still exists, especially in the 5-year LTP trends. Corrected diurnal signatures still exist in the RSS LT time series and in the longer 10-year LTP trends we see a positive bias. Present corrected diurnal signatures are thus likely affecting the long term trend with a warm bias in the RSS data.

Causes of these diurnal errors are due likely to the inability of the climate model, used by RSS, to accurately represent the diurnal cycle or include diurnal variability for

surface temperature [*Dai and Trenberth, 2004; Mears, et al., 2006*]. If the diurnal temperature range has however decreased over time [*Braganza, et al., 2004; LaDochy, et al., 2007*] then a mean diurnal amplitude created from a 5-year time period (1979-1984) will be greater than any diurnal amplitude created after that time period. Using a correction from an earlier time period would over estimate the diurnal correction needed during a later time period. This is what is done by the RSS method and may also be a plausible explanation.

These findings suggest that investigation into the original atmospheric amplification theory and how models handle this theory is necessary. Either the peak in warming is ~300-500 hPa and the theory needs to be revisited, or the theory is correct and climate forcing above this layer is continuing to modify where the peak should be (~200mb). In either case a comprehensive study into what modifies temporal changes in the temperature profile should be at the forefront of future investigations, using the ZTL. How the models are parameterizing these temporal changes need also to be revisited.

Based on these findings the UAH data are likely more accurate (see Chapter 5) and leads to the conclusion that using MSU broad atmospheric weighted channels, in addition to RATPAC(RW), atmospheric amplification is not happening in the atmosphere using globally averaged data over the MSU era. There is evidence however from the radiosonde data, as discussed, that shows greater warming in the ~300-500 hPa layer than at the surface during some LTP in the complete radiosonde database. This temporal change in temperature trends warrants further studies on this subject.

These findings enhance the importance of understanding temporal changes in the atmospheric temperature trend profile. This understanding would lead to further insight into temporal changes in vertically integrated diurnal cycles and implications on multiple climate studies using these data series. It would further aid in the current quest to understand differences between modeled and observed atmospheric amplification.

7.2 Future work

This work indicates temporal changes in temperature trend profiles are not well understood. Their causes are extremely important to improve our understanding of atmospheric changes. Future work should therefore focus on the understanding of these mechanisms in four main areas: atmospheric amplification, ZTL, MSU weighting function and diurnal temperature range. Using LTP appears beneficial and should continue to be useful in future research proposals.

Atmospheric amplification is occurring over most time periods in globally averaged radiosonde data, though not during the MSU era. In addition, the CCSP concluded that models and observations of atmospheric amplification are not in agreement in the tropics, which is in conflict with the current understanding of atmospheric physics. To understand these discrepancies, temporal changes in temperature trend profiles of radiosonde data need to be investigated thoroughly.

The variability of the ZTL is also not understood. Studies into the theoretical radiatively induced ZTL under equilibrium conditions in addition to work understanding forcings causing the variability need to be implemented. These studies would include

model sensitivities to see if the ZTL variability can be reproduced leading to better understanding of forcings in the atmosphere and more accurate model representation.

An additional path of study would use of a static weighting function and how temporal and spatial changes in temperature trends effect interpretation of simulated temperature trends. The temporal change and variability in atmospheric temperature trends are latitude dependent. Using a static weighting does not include latitude dependence of globally averaged trends in the atmosphere and requires further study.

To understand vertically integrated diurnal changes, temporal changes in the atmospheric temperature trend profile need to be investigated at hourly time periods. As shown in this work, diurnal correction to the MSU data leads to the greatest discrepancies between databases. Further work to understand vertically integrated diurnal changes in the atmosphere is paramount to stable MSU data for climate studies.

REFERENCES

- Braganza, K., D. J. Karoly, and J. M. Arblaster (2004), Diurnal temperature range as an index of global climate change during the twentieth century, *Geophysical Research Letters*, *31*.
- Christy, J. R., and W. B. Norris (2006), Satellite and VIZ-radiosonde intercomparisons for diagnosis of nonclimatic influences, *Journal of Atmospheric and Oceanic Technology*, *23*, 1181-1194.
- Christy, J. R., W. B. Norris, R. W. Spencer, and J. J. Hnilo (2007), Tropospheric temperature change since 1979 from tropical radiosonde and satellite measurements, *Journal of Geophysical Research-Atmospheres*, *112*.
- Christy, J. R., and R. W. Spencer (2005), Correcting temperature data sets, *Science*, *310*, 972-972.
- Christy, J. R., R. W. Spencer, and W. D. Braswell (2000), MSU tropospheric temperatures: Dataset construction and radiosonde comparisons, *Journal of Atmospheric and Oceanic Technology*, *17*, 1153-1170.
- Christy, J. R., R. W. Spencer, and R. T. McNider (1995), Reducing Noise in the Msu Daily Lower-Tropospheric Global Temperature Dataset, *Journal of Climate*, *8*, 888-896.
- Christy, J. R., R. W. Spencer, W. B. Norris, W. D. Braswell, and D. E. Parker (2003), Error estimates of version 5.0 of MSU-AMSU bulk atmospheric temperatures, *Journal of Atmospheric and Oceanic Technology*, *20*, 613-629.

Dai, A. G., and K. E. Trenberth (2004), The diurnal cycle and its depiction in the Community Climate System Model, *Journal of Climate*, 17, 930-951.

Folland, C. K., N. A. Rayner, S. J. Brown, T. M. Smith, S. S. P. Shen, D. E. Parker, I. Macadam, P. D. Jones, R. N. Jones, N. Nicholls, and D. M. H. Sexton (2001), Global temperature change and its uncertainties since 1861, *Geophysical Research Letters*, 28, 2621-2624.

Free, M., D. J. Seidel, J. K. Angell, J. Lanzante, I. Durre, and T. C. Peterson (2005), Radiosonde Atmospheric Temperature Products for Assessing Climate (RATPAC): A new data set of large-area anomaly time series, *Journal of Geophysical Research-Atmospheres*, 110.

Fu, Q., and C. M. Johanson (2004b), Stratospheric influences on MSU-derived tropospheric temperature trends: A direct error analysis, *Journal of Climate*, 17, 4636-4640.

Fu, Q., and C. M. Johanson (2005), Satellite-derived vertical dependence of tropical tropospheric temperature trends, *Geophysical Research Letters*, 32.

Fu, Q., C. M. Johanson, J. M. Wallace, and T. Reichler (2006), Enhanced mid-latitude tropospheric warming in satellite measurements, *Science*, 312, 1179-1179.

Fu, Q., C. M. Johanson, S. G. Warren, and D. J. Seidel (2004a), Contribution of stratospheric cooling to satellite-inferred tropospheric temperature trends, *Nature*, 429, 55-58.

Gillett, N. P., B. D. Santer, and A. J. Weaver (2004), Stratospheric cooling and the troposphere, *Nature*, 432.

Grody, N. C. (1983), Severe Storm Observations Using the Microwave Sounding Unit, *Journal of Climate and Applied Meteorology*, 22, 609-625.

Johanson, C. M., and Q. Fu (2006), Robustness of tropospheric temperature trends from MSU channels 2 and 4, *Journal of Climate*, 19, 4234-4242.

Karl, T. R., S. J. Hassol, C. D. Miller, and W. L. Murray (Eds.) (2006), *Temperature Trends in the Lower Atmosphere: Steps for Understanding and Reconciling Differences*, Washington DC.

Kiehl, J. T., J. M. Caron, and J. J. Hack (2005), On using global climate model simulations to assess the accuracy of MSU retrieval methods for tropospheric warming trends, *Journal of Climate*, 18, 2533-2539.

LaDochy, S., R. Medina, and W. Patzert (2007), Recent California climate variability: spatial and temporal patterns in temperature trends, *Climate Research*, 33, 159-169.

Liebe, H. J., G. G. Gimmestad, and J. D. Hopponen (1977), Atmospheric Oxygen Microwave-Spectrum - Experiment Versus Theory, *Ieee Transactions on Antennas and Propagation*, 25, 327-335.

Liebe, H. J., P. W. Rosenkranz, and G. A. Hufford (1992), Atmospheric 60-Ghz Oxygen Spectrum - New Laboratory Measurements and Line Parameters, *Journal of Quantitative Spectroscopy & Radiative Transfer*, 48, 629-643.

Mears, C. A., R. W. Forest, R. S. Spencer, R. W. Vose, and R. W. Reynolds (2006), What is our understanding of the contribution make by observational or methodological uncertainties to the previously reported vertical differences in temperature trends?, in *Temperature Trends in the Lower Atmosphere: Steps for Understanding and Reconciling Differences*, edited by T. R. Karl, et al., A Report by the Climate Change Science Program and the Subcommittee on Global Change Research, Washington, DC.

Mears, C. A., M. C. Schabel, and F. J. Wentz (2003), A reanalysis of the MSU channel 2 tropospheric temperature record, *Journal of Climate*, 16, 3650-3664.

Mears, C. A., and F. J. Wentz (2005), The effect of diurnal correction on satellite-derived lower tropospheric temperature, *Science*, 309, 1548-1551.

Mo, T., M. D. Goldberg, D. S. Crosby, and Z. H. Cheng (2001), Recalibration of the NOAA microwave sounding unit, *Journal of Geophysical Research-Atmospheres*, 106, 10145-10150.

Prabhakara, C., R. Iacovazzi, J. M. Yoo, and G. Dalu (2000), Global warming: Evidence from satellite observations, *Geophysical Research Letters*, 27, 3517-3520.

Randel, W. J., K. Shine, J. Austin, C. Claud, N. P. Gillett, P. Keckhut, U. Langematz, C. Mears, R. Lin, J. Miller, J. Nash, D. J. Seidel, S. Thompson, and S. Yoden (2007), Long-

Term Cooling of the Stratosphere, *Bulletin of the American Meteorological Society*, 88, 620-621.

Randel, W. J., and F. Wu (2006), Biases in stratospheric and tropospheric temperature trends derived from historical radiosonde data, *Journal of Climate*, 19, 2094-2104.

Santer, B. D., T. M. L. Wigley, D. J. Gaffen, L. Bengtsson, C. Doutriaux, J. S. Boyle, M. Esch, J. J. Hnilo, P. D. Jones, G. A. Meehl, E. Roeckner, K. E. Taylor, and M. F. Wehner (2000), Interpreting differential temperature trends at the surface and in the lower troposphere, *Science*, 287, 1227-1232.

Santer, B. D., T. M. L. Wigley, C. Mears, F. J. Wentz, S. A. Klein, D. J. Seidel, K. E. Taylor, P. W. Thorne, M. F. Wehner, P. J. Gleckler, J. S. Boyle, W. D. Collins, K. W. Dixon, C. Doutriaux, M. Free, Q. Fu, J. E. Hansen, G. S. Jones, R. Ruedy, T. R. Karl, J. R. Lanzante, G. A. Meehl, V. Ramaswamy, G. Russell, and G. A. Schmidt (2005), Amplification of surface temperature trends and variability in the tropical atmosphere, *Science*, 309, 1551-1556.

Soden, B. J., D. L. Jackson, V. Ramaswamy, M. D. Schwarzkopf, and X. L. Huang (2005), The radiative signature of upper tropospheric moistening, *Science*, 310, 841-844.

Spencer, R. W., and J. R. Christy (1993), Precision Lower Stratospheric Temperature Monitoring with the Msu - Technique, Validation, and Results 1979-1991, *Journal of Climate*, 6, 1194-1204.

Spencer, R. W., J. R. Christy, W. D. Braswell, and W. B. Norris (2006), Estimation of tropospheric temperature trends from MSU channels 2 and 4, *Journal of Atmospheric and Oceanic Technology*, 23, 417-423.

Spencer, R. W., J. R. Christy, and N. C. Grody (1990), Global Atmospheric-Temperature Monitoring with Satellite Microwave Measurements - Method and Results 1979-84, *Journal of Climate*, 3, 1111-1128.

Stephens, G. L. (1994), *Remote Sensing of the Lower Atmosphere: An Introduction*, 523 pp., Oxford University Press, New York.

Tett, S., and P. Thorne (2004), Tropospheric temperature series from satellites, *Nature*, 432.

Vinnikov, K. Y., N. C. Grody, A. Robock, R. J. Stouffer, P. D. Jones, and M. D. Goldberg (2006), Temperature trends at the surface and in the troposphere, *Journal of Geophysical Research-Atmospheres*, 111.

Wigley, T. M. L. (2006), Appendix A: Statistical issues Regarding Trends, in *Temperature Trends in the Lower Atmosphere: Steps for Understanding and Reconciling Differences*, edited by T. R. Karl, et al., A Report by the Climate Change Science Program and the Subcommittee on Global Change Research, Washington, DC

Zou, C. Z., M. D. Goldberg, Z. H. Cheng, N. C. Grody, J. T. Sullivan, C. Y. Cao, and D. Tarpley (2006), Recalibration of microwave sounding unit for climate studies using simultaneous nadir overpasses, *Journal of Geophysical Research-Atmospheres*, 111.